Design and Development of a High Performance Zinc Air Fuel Cell

Dewald Lourens

20040997

A dissertation submitted in fulfillment of the requirements for the

Magister Technologiae: Engineering: Electrical

Department: Applied Electronics and Electronic Communication

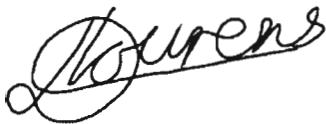**Faculty of Engineering**

Vaal University of Technology

Vanderbijlpark

Supervisor: Prof HCvZ Pienaar

Date: June 2006

Declaration

I, Dewald Lourens, hereby declare that the following research information is solely my own work. This is submitted for the requirements for the Magister Technologiae: Engineering: Electrical to the Department of Applied Electronics and Electronic Communication at the Vaal University of Technology, Vanderbijlpark. This work has not previously been accepted in substance for any degree and is not being concurrently submitted in candidature for any degree.

03-08-2006

Acknowledgements

I hereby wish to express my gratitude to the following individuals who enabled this document to be completed successfully:

Abstract

The demand for efficient and environmentally friendly power sources has become a major topic around the world. This research explores the capability of the zinc-air fuel cell to replace conventional power sources for various applications, more specifically telecommunication systems.

The research consisted of a theoretical study of the zinc-air fuel cell and its components, as well as their performance characteristics. A zinc-air fuel cell and test rig were built, and the system was tested under various conditions.

It was found that the zinc-air fuel cell has an advantage over other fuel cells in that it does not require any expensive materials or noble metals, reducing the overall cost of such a system. The fuel cell showed the potential to power various applications, but problems persisted in the fueling process as well as constant leaking of the aqueous electrolyte.

TABLE OF CONTENTS

List of figures

List of tables

Annexures

.

Glossary of abbreviations and symbols

A

Al – Aluminum
AMS – Advanced Membrane Systems
amu – atomic mass unit

B

BET – Brunner Emmet Teller

C

C – Carbon atom
C - Celsius
C – Coulomb
CAD – Computer aided design
cm – 10^{-2} meter
CO_2 – Carbon dioxide

D

ΔG_f – Charge in gibbs free energy of formation
$\Delta \overline{g}_f$ - per mole change in gibbs free energy of formation
DC – Direct current
DMFC – Direct methanol fuel cell

E

E^0 – Theoretical fuel cell electromotive force
e – electron
EMF – Electromotive force

F

F – Faraday constant, 96 485 Coulomb
F – Fluorine
FC – Fuel cell
Fe - Iron

G

g – gram
G_f – Gibbs free energy of formation
GDE – Gas Diffusion Electrode
GPE – Gas Permeable Electrode

H

h - hour
H – Hydrogen atom
H_2 – Hydrogen molecule
H_2O – Water molecule

I

ICD – In circuit debugger
ICE – Internal combustion engine

J

J - Joule

K

K - Kelvin
K_2CO_3 – Potassium carbonate
KOH – Potassium hydroxide

L

Li - Lithuim

M

m – meter
m – milli, 10^{-3}
min - minute
mm - Millimeter

Mg - Magnesium

N

N – Avogadro's number, 6.022×10^{23}
N – Nitrogen atom
N_2 – Nitrogen molecule
Ni - Nickel
NaOH – Sodium hydroxide

O

Ω - Ohm
O – Oxygen atom
O_2 – Oxygen molecule
OH^- - Hydroxyl ion
O_2H^- - Peroxide

P

PCB – Printed circuit board
PEMFC – Proton Exchange Membrane Fuel Cell
PTFE – Polytetrafluoroethylene
PVC – Polyvinyl chloride

Q

q – Charge of an electron, 1.602×10^{-19} C

R

R - Resistance
R&D – Research and Development

RH – Relative humidity

S

s - second
SEM – Scanning electron microscope

T

T - Temperature

U

μ – micro, 10^{-6}
UPS – Uninterruptible power supply

V

V – Volt

W

W - Watt

XYZ

Zn – Zinc
ZnO – Zinc-oxide

Chapter 1   Introduction

1.1 Background

Probably the two biggest concerns with conventional energy sources are the amount of pollutants that are released into the atmosphere and the efficiency of these systems to convert energy. An example of this is the internal combustion engine (ICE) which is only about 17 percent efficient. Growing concerns over environmental changes caused by power generation with fossil fuels has lead to the development of alternative energy sources that are highly efficient and pollution free. The need for safe and environmentally friendly power has become one of the main topics around the world. Soaring oil prices have also led to an increase in the research and development (R&D) of these systems.

Stationary applications requiring fossil fuels has been replaced with environmentally friendly renewable energy sources such as solar panels and wind turbines. Although cheap and clean, they suffer from the limitations in that they can only operate at certain conditions and still require the addition of battery banks for energy storage. An alternative to renewable energy sources could be fuel cells.

Fuel cells are devices that convert chemical energy directly into electrical energy thus increasing the efficiency of energy conversion. Fuel cells have efficiency levels up to 55% compared to the 35% of conventional power plants (Edugreen.teri..res.in/, 2006). One major disadvantage of most fuel cells is cost due to the noble metal catalysts that are required. However, the zinc-air fuel cell does not require any noble metals.

Successful commercialization of zinc-air cell technology was demonstrated in the 1930s when it was first used for railway signalling. Since then much research has been done on this technology. For applications such as remote telecommunication sites where power is necessary, zinc-air cells show great promise compared to the

1

large battery banks currently used and other expensive fuel cells currently under development.

A power supply that might meet the technical requirements of telecommunication systems is the zinc-air fuel cell. Although zinc-air batteries are common these days, the design of a zinc-air fuel cell is more involved. A clear definition of a zinc-air fuel cell is given on page 43. Design of the zinc-air fuel cell has been attempted many times, but never commercialised. The system proposed within this document pursues a different approach to that followed by other researchers. Problems encountered with the design of such a system are the zinc fuel feed. Unlike other fuel cells, zinc-air fuel cells can not be supplied by a common fuel feeding system due to the conductance of the metal fuel, which shorts all the cells.

1.2 Problem statement

There is a need for a fuel cell system that can power a 100 W telecommunication system for one month. A zinc-air battery system consisting of 80 Ah cells would require a battery bank of more than a 1 000 cells. However preliminary calculations by the researcher indicated that this figure could be greatly reduced by a novel design of this fuel cell system. Hence this attempt to design a smaller more economical fuel cell system.

1.3 Methodology

The research was divided into three phases. The first phase consisted of a theoretical study of the zinc-air fuel cell and the performance characteristics thereof. The second phase was a combination of practical design and theory. This phase dealt with the design and development of a zinc-air fuel cell system. The third and final phase was the testing of the zinc-air fuel cell system.

1.4 Delimitations

The 100 W fuel cell stack model was based on the results obtained from a single zinc-air fuel cell. Power losses and self discharge due to auxiliary components and the joint electrolyte feed were not considered in the model. The bi-functional GDE will also not be considered because fuel cells are not electrically rechargeable batteries.

1.5 Importance of the research

Due to the remote location of some telecommunication systems, reliable and efficient power systems are required. These sites currently use a combination of solar panels and battery banks as power supplies. Both these systems have disadvantages. Solar panels are constantly stolen at these sites while the cycle cost of batteries surpasses that of fuel cells over time. For this reason, telecommunication systems require a new type of cheap, reliable and environmental friendly alternative power source.

The results of this research can shed some light on the technology and design of zinc-air fuel cell systems. Furthermore, zinc-air fuel cells have additional advantages over other fuel cell technologies such as cost and safety. The project will also provide a design of a prototype system, to prove the capability of such a system to power various applications, especially telecommunication systems.

1.6 Overview of the report

Chapter 2 starts with an introduction to the history of the zinc-air cell after which the operation of such a cell is explained. This is followed by an exposition of the different components within the zinc-air cell. A theoretical study of these components will familiarise the reader with the technology. The performance characteristics of a fuel cell as well as the different conditions and environmental factors that influence the operation and performance of the cells are discussed.

3

Chapter 3 deals with the design and development of the system. Due to some confusion in terminology, a clear definition is formulated for the zinc-air fuel cell. The design process was divided into separate sections, starting first with the design of the cell itself, and then the auxiliary systems such as the fuelling mechanism, electrolyte circulation system and the electronic control unit. All of these auxiliary systems are required for the system to operate correctly.

Chapter 4 reports various experiments that were carried out on the system. All the results are discussed and interpreted.

In Chapter 5, conclusions are drawn from the study on the zinc-air fuel cell and recommendations are made regarding the design. Problems encountered during the design are also discussed and possible solutions presented. Additional research suggestions are also made by the researcher that may be of benefit to fuel cell technology.

1.7 Summary

In this chapter the underlying factors that inspired the need for the research as well its importance and relevance, were presented. The research methodology was described and an overview of the report was given. It was stated that the study is on zinc-air fuel cell power sources for remote telecommunication systems. The next chapter will cover a theoretical study of the zinc-air cell, its components and factors that influence the performance of such a system.

Chapter 2   Study of zinc-air technology

2.1   Introduction

According to Bender, Cretzmeyer and Reise (1995:1) atmospheric oxygen was first explored in the nineteenth century as a depolarizing agent for electrochemical systems. It was the work of Maiche who in 1878 replaced the manganese dioxide cathode of the Leclanché cell with a porous platinised carbon/air electrode, but technological limitations prevented the zinc-air battery from commercialization until 1930. In 1932 Heise and Schumacher constructed alkaline electrolyte zinc-air cells with porous carbon air electrodes impregnated with wax to prevent flooding (the overflow of the aqueous solution into the pores of the electrode). This design to date has almost stayed unchanged for the manufacturing of large industrial zinc air batteries.

According to Vincent and Scrosati (1997:98) metal-air batteries owe their technological advances to the research that was carried out in the 1960's on high current density air electrodes for hydrogen/oxygen fuel cells using aqueous electrolytes. It was around this time that America and Russia was locked in the race to the moon. Bender *et al.* (1995:1) goes on to say that fuel cell research for the space programs made the thin, efficient air cathodes used today possible, through the emergence of fluorocarbons as a polymer class. The hydrophobicity combined with the gas porosity of these materials, made it possible to develop thin, high performance gas electrodes using a Teflon bonded catalyst structure and a hydrophobic cathode structure.

According to Bender *et al.* (1995:1) the first zinc-air batteries were used as power sources for remote railway signalling and navigation aid systems. Since then, zinc-air technology has come a long way and today applications range from small electronic appliances such as hearing aids to larger power units like vehicles and

busses. The most common zinc-air battery in use today is the miniature button cell while larger primary zinc-air batteries are available for specialized applications.

Technological advances in the carbon air electrode has led researchers to re-evaluate the potential of the zinc-air battery and fuel cell as a alternative power source to the more conventional batteries and expensive fuel cells. According to Zhu *et al.* (2003:29) zinc-air batteries were not commercially feasible until the development of Teflon, which allowed the oxygen electrode to operate efficiently. According to Wei *et al.* (2000:83) the major breakthrough was the development of various alternative catalysts as replacements to platinum in the air cathodes. The current alternatives are manganese dioxide, cobalt tetramethoxy porphorin and perovskite-type oxides. The use of these alternative catalysts have reduced the cost of development and bought about renewed excitement in this technology.

According to Bender *et al.* (1995:14) there are four mechanisms that affect the capacity of a zinc-air cell during storage and operating service. One of the mechanisms is the self-discharge of the zinc, which is an internal reaction while the other three are caused by gas transfer. Direct oxidation of the zinc anode, carbonation of the electrolyte and water gain or loss by the electrolyte are all causes of gas transfer.

Compared to conventional batteries and fuel cell systems, zinc-air technology shows great promise as an alternative power source to both these systems. Zinc-air technology holds the advantage of being lighter and occupying less space than the conventional lead-acid battery, with the added advantage of containing no environmentally hazardous waste products. Compared to fuel cells they are less expensive and do not require any flammable fuel such as hydrogen.

Academics are primarily focussing their research on the components of the electrically rechargeable zinc-air cell, the most important being the development of bi-functional air electrodes with improved catalytic properties and reaction kinetics

as well as increased operational life. Another important component being researched is the zinc electrode, which suffers from radical shape changes and dendrite formation under normal cycle conditions, limiting the cycle life of the cell. Industry is focussing their effort on the development of cheap reliable primary zinc-air cells for uninterruptible power supply (UPS), electric busses, vehicles and military use. Some companies are also researching the possibility of a regenerative zinc-air fuel cell system for UPS's.

In this chapter, the operation of the zinc-air cell and its different components will be explained. This chapter will also look at the electrical characteristics of a zinc-air cell and the effects of various environmental changes on its performance.

2.2   Operation of the zinc-air cell

Although there are four different types of zinc-air cells under development and some in commercial use today, they all operate on the same basic principle. The four different types are the primary cell, secondary cell, mechanically rechargeable cell and lastly the fuel cell. The zinc-air cell works like a conventional battery in that it generates electrical energy by converting chemical energy into electrical energy by means of an electrochemical reaction. The major difference between the zinc-air cell and conventional batteries is that the zinc-air cell gets one of its main reactants, oxygen, from the surrounding air.

Electrical energy is generated when oxygen molecules from the atmosphere enter the gas diffusion electrode. Here, the oxygen molecules split into individual oxygen atoms and water, already present in the pores of the electrode, reacts with the oxygen atoms to form hydroxyl ions. The hydroxyl ions migrate through the electrolyte and the physical separator to the zinc anode, where each hydroxyl ion binds to a zinc atom to produce zincate and two free electrons. The zincate immediately splits into two hydroxyl molecules, one water molecule and one zinc-oxide molecule. The free electrons move from anode to cathode through an external load. Figure 1 shows a graphic representation of the reactions taking place on a molecular level.

7
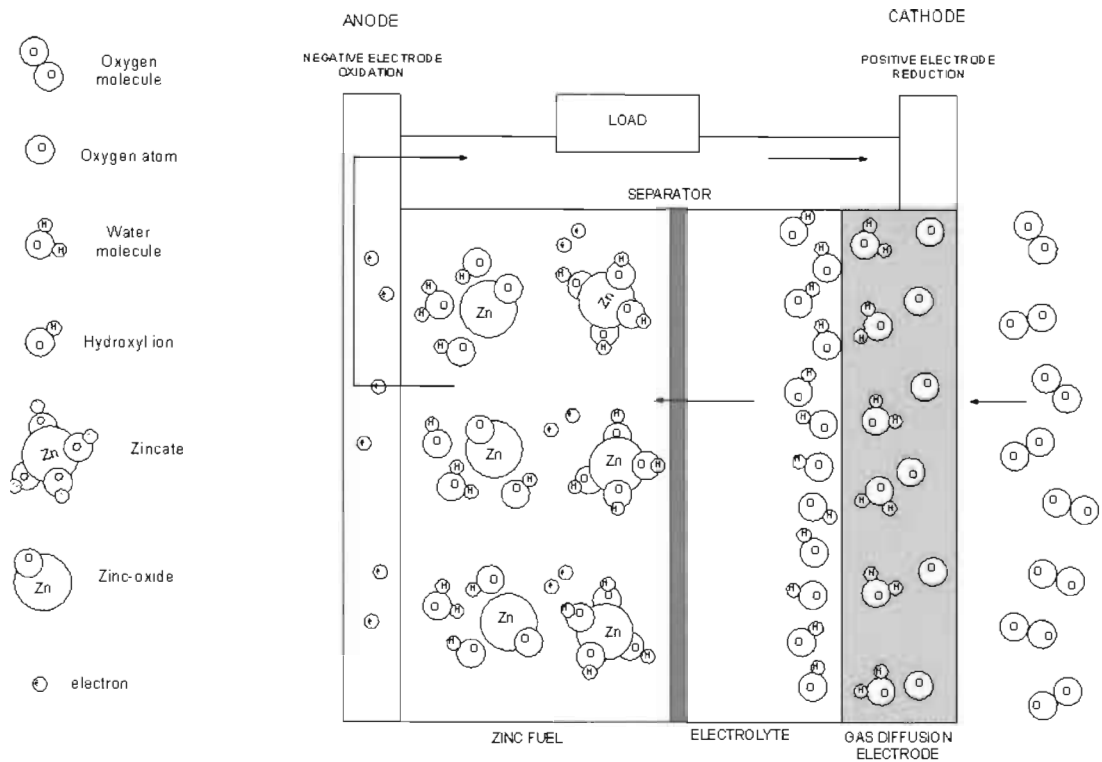
Figure 1: Operation of a zinc-air cell.

The reactions that take place at the individual electrodes are as follows:

At the cathode: $\frac{1}{2} O_2 + H_2O + 2e \rightarrow 2OH^-$ $E^0 = 0.40$ V

At the anode: $Zn \rightarrow Zn^{2+} + 2e$

$Zn^{2+} + 2OH^- \rightarrow Zn(OH)_2$ $E^0 = 1.25$ V

$Zn(OH)_2 \rightarrow ZnO + H_2O$

Overall reaction: $Zn + \frac{1}{2} O_2 \rightarrow ZnO$ $E^0 = 1.65$ V
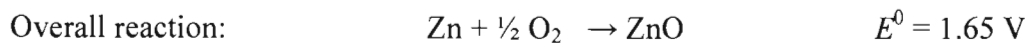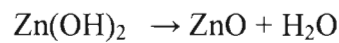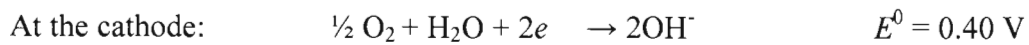
2.3   Components

A typical zinc-air cell consists of the following components: a gas permeable electrode (GPE) or gas diffusion electrode (GDE) at the cathode, a solid porous zinc anode or zinc slurry at the anode, an ion conducting electrolyte and some form of mechanical separator to prevent short circuiting between the anode and cathode.
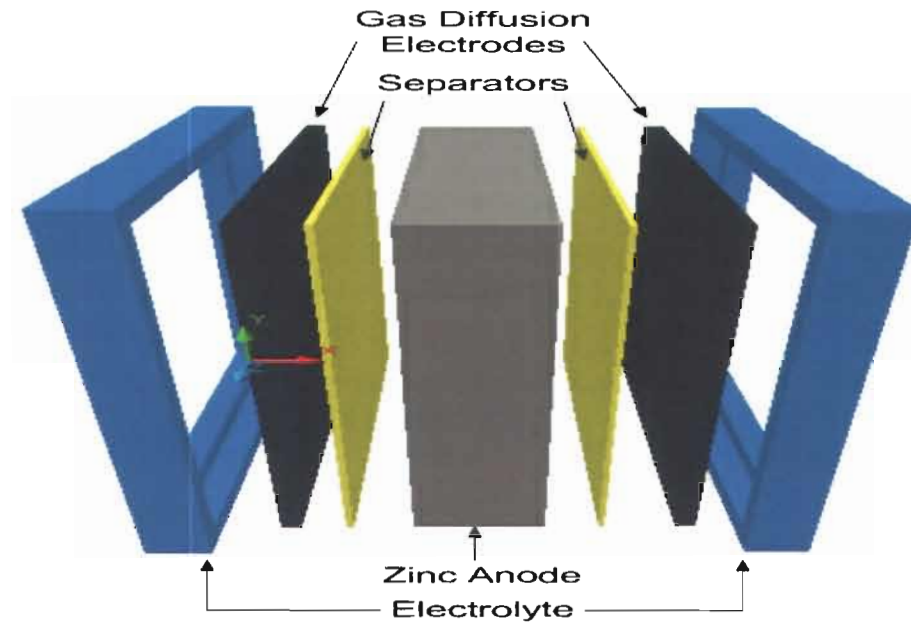
Figure 2: Structural layout of a zinc-air cell.

2.3.1   Gas Diffusion Electrode (GDE)

The GDE which forms the positive component of a zinc-air cell undergoes oxygen reduction and is thus termed the cathode. The GDE used in alkaline fuel cell systems are basically the same as that used in all metal-air batteries and metal-air fuel cells, the only difference being the type of catalyst used. Kaisheva (2004:1) provides two advantages over the metal-oxide cathode used in conventional primary batteries: infinite charge capacity and low weight independent of the capacity. For this reason, zinc-air cells are capable of delivering more energy per weight and volume than most other batteries.

The two basic structures used for GDE are: (1) the carbon based electrode with hydrophobic surface and (2) the metal based electrode with a hydrophilic surface. Since the discovery of fluorocarbons such as polytetrafluoroethylene (PTFE), modern electrodes tend to use carbon based electrodes rather than the old heavier metal based electrodes.

Gas

Carbon
particle

Wet proofing
agent

Electrolyte

Hydrophobic properties
in pores
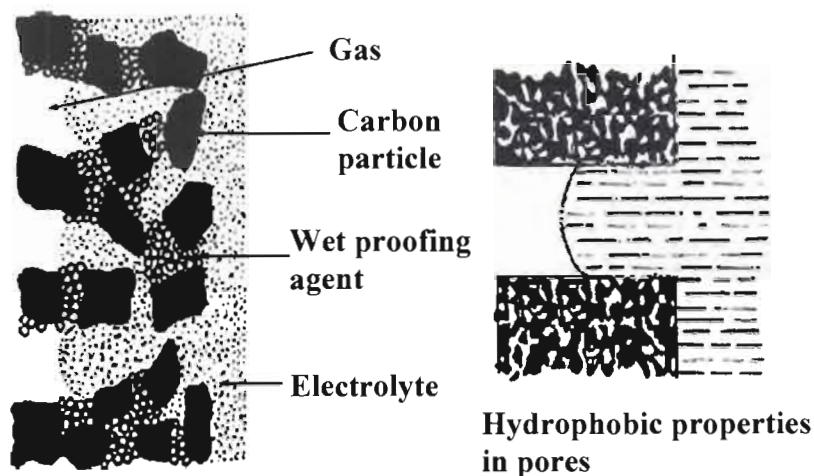
Figure 3: Section view of a hydrophobic gas diffusion layer (Kordesch & Hacker 2003:766).

Hydrophobic GDE's (Figure 3) are manufactured from fine carbon powders bonded with a wet proofing agent, usually PTFE. The advantages of using carbon powders are that they are lightweight, have a large surface area and are suitable for very active catalyst deposition. To improve the conductivity of these electrodes, a wire screen is added as current collector (Kordesch & Hacker 2003:765). The wire screen also gives additional strength to the otherwise weak electrode structure.

The PTFE not only acts as a binder, but its hydrophobic properties stop the electrode from flooding and provide for a controlled permeation by the liquid electrolyte. An additional layer of PTFE is put over the surface of the electrode to further control the porosity and to prevent the electrolyte from leaking through the electrode. This is done without the need to pressurize the reactant gases, as has to be done with metal-based electrodes (Larminie & Dicks 2003:135). Another characteristic of PTFE is the strong bonds formed between the fluorine and the carbon making it durable and resistant to chemical attack (Larminie & Dicks 2003:70).
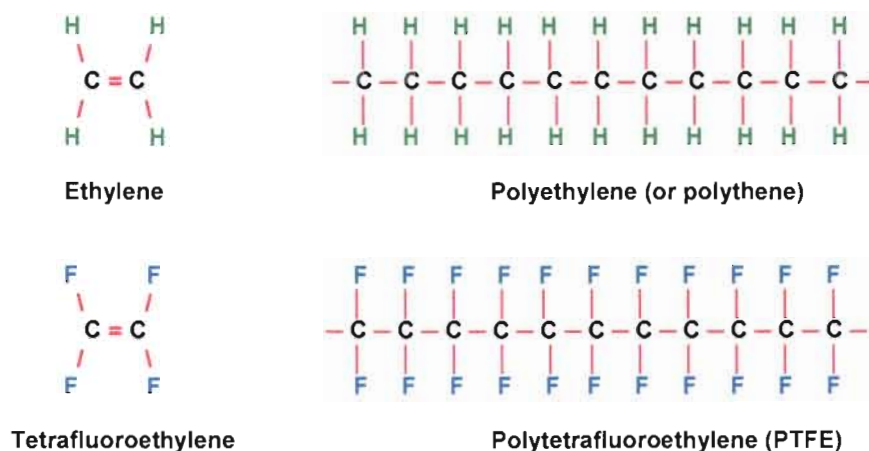
Figure 4: Molecular structures of different polymers (Larminie & Dicks 2003:70).

PTFE is constructed by starting with the simplest man-made polymer, polyethylene. The polymer is then modified by substituting the hydrogen by fluorine, this process is called perfluorination. The modified polymer formed is called polytetrafluoroethylene or PTFE. The molecular structures of the different polymers are shown in figure 4 (Larminie & Dicks 2003:69). PTFE (better known as Teflon) was discovered by accident in 1938 by Du Point chemist, Roy Plunkett (Packagingtoday.com, 2006).

Hydrophilic GDE's (Figure 5) are made from sintered metal powders, which have larger pores at the gas diffusion layer than at the reaction layer. This requires capillary forces to keep the electrolyte in the small pores when an overpressure of the gasses with respect to the electrolyte is applied. Porous metal electrodes are heavy, but have the advantage of having a high conductivity which is good for monopolar plate electrodes where the current is drawn from tabs at the edges of the electrodes. Raney metal structures provide high catalytic activity at low temperatures without using platinum (Kordesch & Hacker 2003:766).
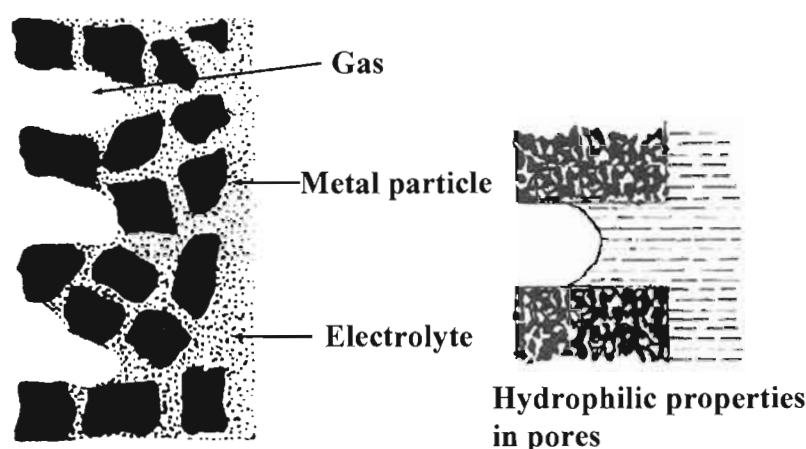
Figure 5: Section view of a hydrophilic gas diffusion layer (Kordesch & Hacker 2003:766).

Raney metals are prepared by mixing an active metal, called the host metal (e.g. nickel), with an inactive metal, usually aluminium. The mixing of the two metals is done in such a way that they maintain their distinct regions of aluminium and the host metal. Treatment with a strong alkali then dissolves the aluminium, resulting in a porous material with a very high surface area. The host metals are usually Raney nickel for the anode and Raney silver for the cathode (Larminie & Dicks 2003:134). The reasons for the two different metals are that nickel has better catalytic properties on hydrogen and silver on oxygen. This is used in alkaline fuel cells.

A recent development in carbon based GDE is the bi-functional GDE used in electrically rechargeable zinc air batteries. These electrodes are capable of oxygen reduction during discharge and oxygen evolution during charging. According to Chakkaravarthy *et al.* (1981:219) the electrode consists of two zones connected to a common metal grid. The two zones are the charging zone that is hydrophilic with respect to the electrolyte, and a discharging zone that is hydrophobic with respect to the electrolyte.

Budesvski (2003:1320) explains that as an air electrode, carbon based GDE has an operating life span at room temperature of between 8 000 and 10 000 hours at

200 mA.cm^{-2}. Carbon-based GDE's also perform well at low temperatures down to - $10\,^{\circ}C$ and are insensitive to the presence of CO_2.

For the purpose of this research only carbon based electrodes will be considered. The reasons for this are:

- Prevention of the electrolyte leaking through electrode is simple, unlike the careful control of differential pressures required when using metal based electrodes.
- Light weight, increasing the specific energy density of the system.
- Low cost materials.

2.3.1.1 Materials

The most widely used GDE is carbon based. These electrodes make use of a wide variety of carbon materials such as graphite, carbon blacks and carbon substrates. Current research is directed to the development of carbon based nanotubes as catalyst carriers in fuel cells.

Electrochemical systems use natural graphite such as Lonza KS44, Brunner Emmet Teller (BET) with a surface area of 9 m^2.g^{-1} and artificial graphite such as Asbury Micro #250 and BET with a surface area of 22 m^2.g^{-1}. The production of carbon fibers, cloths and felts by solid-phase pyrolysis of non-melting polymers are used as substrates for gas electrode backing material current collectors (Kordesch & Hacker 2003:767).

Carbon blacks are distinguished by their surface area, particle size, oil absorption, volatile content, pH, electrical resistivity, density and extent of graphitization. Their surface areas range from between 25 and 2000 m^2.g^{-1} with densities varying from 1,9 g.cm^{-3} to below 1,4 g.cm^{-3} for gas activated carbon blacks. Electrical resistivity varies from 0,001 to 1 Ω.cm. The most common carbon blacks are

Acetylene black, Vulcan XC-72R and Black Pearls 2000 (Kordesch & Hacker 2003:767).

Conductive carbon substrates such as carbon paper, cloth or felt are tailor made for use in fuel cells containing no plastic binders after carbonization. The substrates are made hydrophobic prior to use by adding layers of Teflon (Kordesch & Hacker 2003:767).

(i)   (ii)
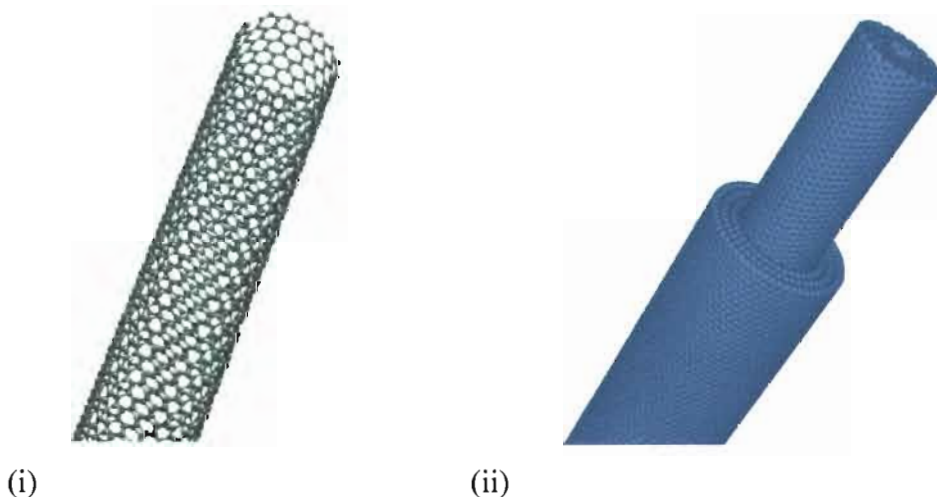
Figure 6: (i) A single-walled nanotube (Ewels 2005), and (ii) a multi-walled nanotube (Pescovitz 2002).

It is likely that future technology will make use of nano-technology in the manufacturing of GDE's, since catalyst carrier carbon nanotubes could provide higher chemical and mechanical stability, higher electrical conductivity and increase the reaction inter phase. Carbon nanotubes are said to have one hundred times the tensile strength of steel, thermal conductivity better than all but the purest diamond and electrical conductivity similar to copper, but with the ability to carry much higher currents (Budevski 2003:1323). Figure 6 shows a schematic representation of a (i) single-walled and (ii) multi-walled nanotube.

2.3.1.2   Catalytic Properties

According to Kaisheva and Milusheva (2004:1) catalytic acceleration of the electrochemical reduction of oxygen is of the greatest importance when using GDE's in fuel cells and metal-air cells, because without an appropriate catalyst, it is impossible to attain the high current densities required to meet the technical demands of modern appliances.
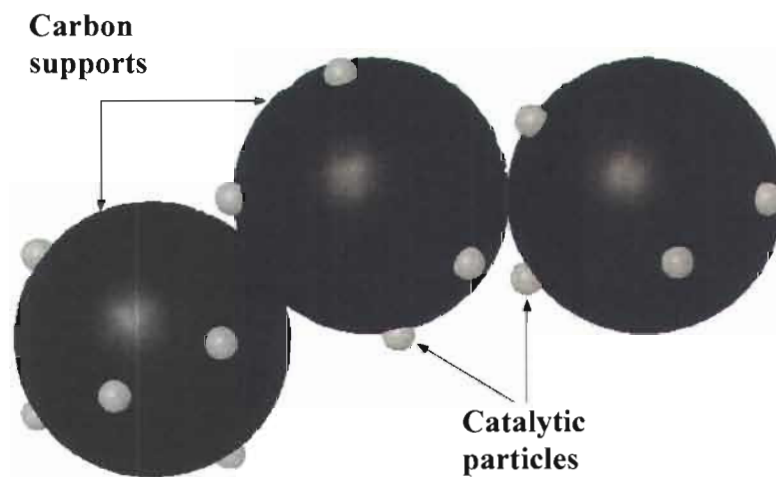
Figure 7: Idealised structure of a carbon supported catalyst (Larminie & Dicks 2003:72).

Bender *et al.* (1995:2) explain that a rate limiting step exists within the reaction chemistry that affects the reaction kinetics and hence the performance of the zinc-air cell. This relates to the oxygen reduction process, wherein peroxide-free radical (O_2H^-) formation occurs. The rate limiting reactions:

Step 1 $O_2 + H_2O + 2e \rightarrow O_2H^- + OH^-$

Step 2 $O_2H^- \rightarrow OH^- + \frac{1}{2} O_2$
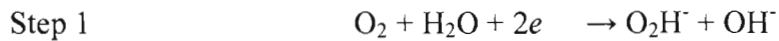
Decomposition of the peroxide to hydroxide and oxygen is a key rate-limiting step in the reaction. The reduction of the peroxide species and the overall reaction rate can be accelerated by the addition of catalytic compounds which promote the reaction in step 2 (Bender *et al.*, 1995:3).

The most common catalyst used in fuel cells is platinum, but for the zinc-air battery, manganese can be used to accelerate the reaction at the cathode. Figure 7 shows the structure of an idealised carbon supported catalyst (Larminie & Dicks 2003:135). Bender *et al.* (1995:3) go on to say that catalyst used in zinc-air batteries are typically transition metal compounds such as oxides and organometallic complexes, noble metals and their compounds, as well as mixed metal compounds, including rare-earth metals. The use of non-noble metals for catalytic acceleration is a major advantage in the design of a zinc-air fuel cell, because it reduces overall cost.

2.3.1.3   Three-phase boundary
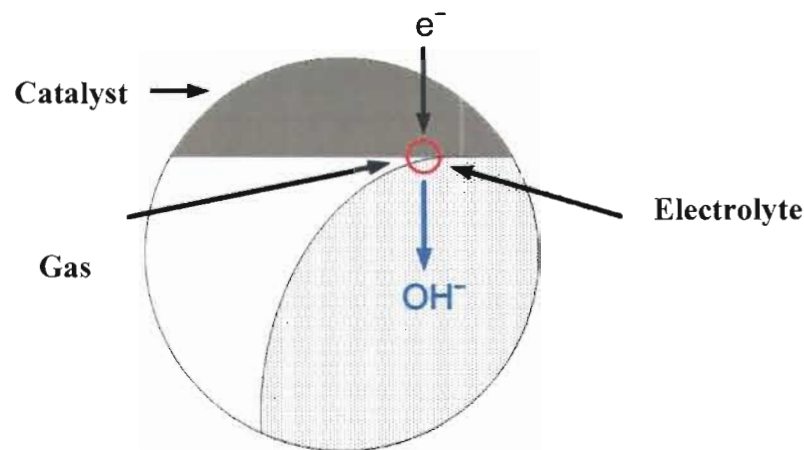
Figure 8: Three-phase boundary (Budevski, 2003:1320).

To fully understand the working of the GDE, it must be viewed from a molecular level. Vincent and Scrosati (1997:99) explains that the electrode reaction can only take place in the region where solid, liquid and gaseous phases come together.

Therefore, the construction of the oxygen electrodes is designed to maximize the interfaces between these phases. The region where the three phases interface is commonly known as the three-phase boundary (Figure 8).

The three-phase boundary, as shown in figure 8, is the point (red circle) at which all three phases are in contact with each other. Oxygen molecules from the air react with the electrolyte and electrons to form hydroxyl ions. Vincent and Scrosati (1997:99) state that the oxygen consumption at the air electrode is 0,058 $cm^3.C^{-1}$ which corresponds to $5,8 \times 10^{-5}$ $cm^3.s^{-1}$ for a 1 mA discharge.

2.3.1.4   Environmental effects

An important factor that reduces the lifetime of a carbon supported GDE is the presence of CO_2 in the air, because CO_2 reacts with the potassium hydroxide electrolyte to produce potassium carbonate solids that block the pores of the GDE. Another factor that may also have an impact on the operational lifetime is thermal expansion between the carbon and the metal grid of the GDE. This section will elaborate on theses effects.

Berndt (1997:64) explains that the aqueous electrolyte, potassium hydroxide, is not stable when exposed to CO_2 containing air, which is gradually converted into potassium carbonate (K_2CO_3), forming white crusts of crystals.

The formation of carbonate crystals blocks the pores of the GDE, reducing the rate at which oxygen diffuses through the electrode, up to the point where no more oxygen gets diffused through the electrode. This makes the electrode useless and halts the chemical reactions. Figure 9 shows different degrees of carbonation and how it affects the diffusion of oxygen through the electrode.

Carbon supported GDE has been shown to have an operational lifetime of between 1600 to 3600 hours at 65 °C at 100 $mA.cm^{-2}$ when using air containing CO_2. When

CO_2-free air was used under similar conditions, the lifetime was increased to more than 4000 hours (Larminie & Dicks, 2003:136).

Air   Electrolyte

No blockage →

Partial blockage →

Potassium carbonate

Complete blockage →
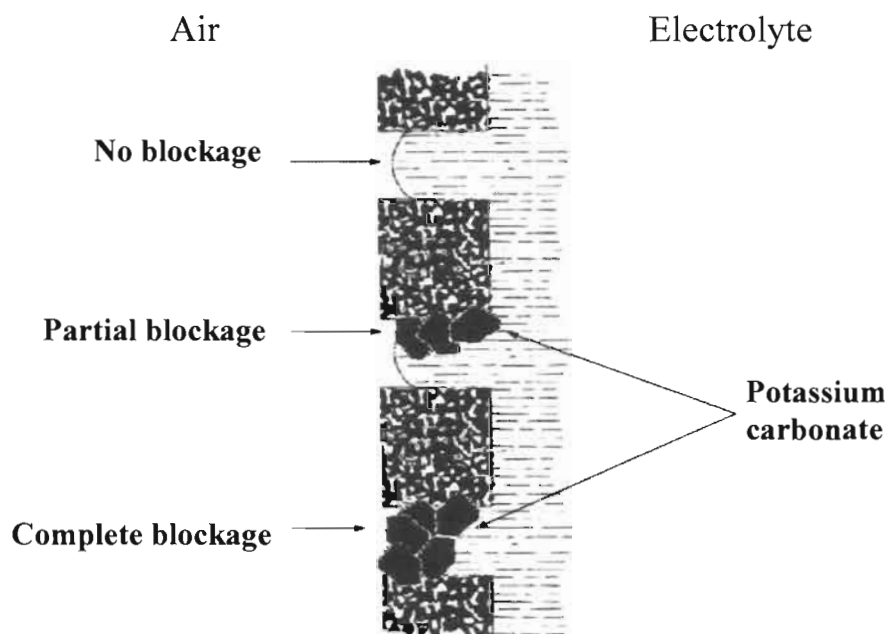
Figure 9: Carbonate formation in the pores of a hydrophobic GDE.

Temperature fluctuations affect the physical structure of the GDE. Thermal expansion differences between both the carbon and metal current collector could cause cracks to form in the GDE, which can result in leakage through the electrode. The main reason for this is poor matching of expansion coefficients. The life expectancy of metal screen containing electrodes is considerably lower than that of single structured electrodes of only carbon (Kordesch & Hacker, 2003:767).

Maximum operational lifetime of a carbon based GDE can only be attained by; either some form of CO_2 filter or scrubber or the use of pure oxygen as the feed gas. Leaking that occurs due to thermal expansion differences can be prevented by minimizing temperature fluctuations within the system or by better matching of expansion coefficients. Another alternative will be to discard the metal current collector altogether. The latter is not advised as this will greatly affect the conductivity, performance and overall strength of the cell.

18

2.3.1.5 Function

The functions of the GDE in a zinc-air cell can be summarised as follows:

- Confines of the liquid electrolyte separating the gaseous oxygen and the solid zinc.
- Facilitates a highly developed three phase boundary where gas, liquid and solid interface.
- Serves as a carrier of the catalyst ensuring a fast electron exchange reaction (Budevski, 2003:1319).
- Provides fast transportation of the reactants and the reaction products to and from the three phase boundary (Budevski, 2003:1319).
- Ensures fast lateral electron transportation (Budevski, 2003:1319).
- Gives stability and strength to the prismatic cell.

2.3.2 Zinc Electrode

Various types of metals can be used as fuel in both metal-air batteries and metal-air fuel cells. These include aluminium, iron, lithium, magnesium and zinc, all of which have shown potential, but all with different degrees of success. Table 1 shows how these metals measure up to each other with respect to their energy density per weight of metal fuel. Although zinc has one of the lowest energy densities, it is the most widely used and researched of all metal-air fuel. Zinc fuel refers to the zinc metal used in the zinc-air cell and this terminology will be used throughout this dissertation.

Metals that have been extensively studied for use in metal air batteries and fuel cells are: zinc, aluminium, magnesium and lithium. The last three metals suffer from severe corrosion problems during storage. Aluminium-air and magnesium-air systems are generally operated as reserve systems where the electrolyte is added when required, or as mechanically rechargeable batteries which have replacement

anodes. Zinc compensates for its lower power and energy density by the ease with which the corrosion process can be inhibited (Vincent & Scrosati, 1997:100).

Table 1: Properties of various metals used in metal-air batteries (Dobley *et al.*, 2005).

Anode	Ah.g^{-1}	Theoretical Voltage	Theoretical kWh.kg^{-1}
Li	3,86	3,4	13,0
Al	2,98	2,7	8,1
Mg	2,20	3,1	6,8
Zn	0,82	1,65	1,37
Fe	0,96	1,3	1,2

Suresh Kannan *et al.* (1995:93) list some criteria of a good battery anode as follows:
- High negative open-circuit potential,
- Zero or negligible corrosion rate,
- Minimal polarization,
- Very high utilization efficiency,
- Environmentally safe manufacturing of anode and electrolyte, and
- competitive cost of cell production.

Of all the possible materials that can be considered for the anode electrode, zinc best suites the criteria listed above.

2.3.2.1   Zinc as fuel

As an energy storage material, metallic zinc has excellent electrochemical properties with fast electrode kinetics and a high overpotential towards the hydrogen evolution. Although the transformable free energy (ΔG) of zinc is only 1,37 kWh.kg^{-1} compared to 33 kWh.kg^{-1} for hydrogen (based on the molecular weight of the fuels), it has a energy density about four times that of liquid hydrogen or 11 times that of compressed hydrogen at 300 bar (Haas *et al.*, 2003:383).

Another advantage is that zinc can be reconverted back to pure zinc. This bought about the design of electrically rechargeable zinc-air cells and proposed regenerative plants where the zinc anodes of mechanically rechargeable zinc-air cells can be replaced while the spent electrode can be recharged externally.

Electric-fuel.com (1995) proposed a recharging and recycling process as follows:

- Disassembly. This involves the removal of the zinc oxide discharged product (anode).

- Dissolution. The zinc oxide is dissolved in a KOH solution to form a zincate rich feed, according to the equation:

$$ZnO + 2KOH + H_2O = K_2Zn(OH)_4 \qquad (2.1)$$

- Electrowinning. The process whereby the zincate solution is electrolyzed in an electrowinning bath to form zinc, this is shown by the following equation:

$$K_2Zn(OH)_4 = Zn + 2KOH + H_2O + \tfrac{1}{2} O \qquad (2.2)$$

- Reassembly. The process whereby the electro won zinc is compacted onto a current collector frame and inserted into its separator.

2.3.2.2   Structure

Zinc fuel currently exists in two forms, namely: A planar electrode (figure 10) used in most primary, secondary and mechanically rechargeable zinc-air cells and a form of zinc slurry or pellets, used usually in the design of a zinc-air fuel cell where the fuel can be circulated through the system, constantly replenishing the cells.
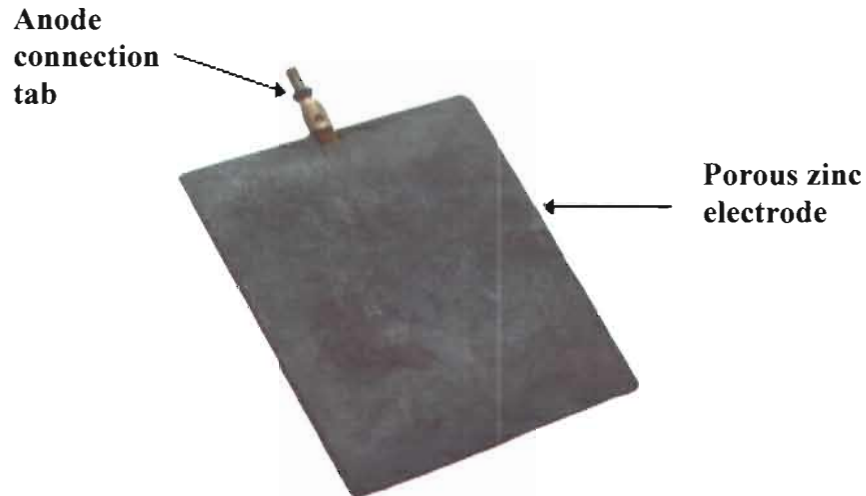
Figure 10: Photograph of a porous planar zinc electrode.

The planar zinc electrode is manufactured using very high purity (99, 9%) zinc. According to Jiang and Cintra (Freshpatents.com, 2005) the method of forming an anode is as follows:

- Mix the zinc particles with binders and water to form a wet paste.
- Mould the wet paste to the desired shape and heat it to evaporate the water. A solid mass is formed with a network of microscopic void spaces between the particles. The void spaces that form allow the electrode to absorb the electrolyte.
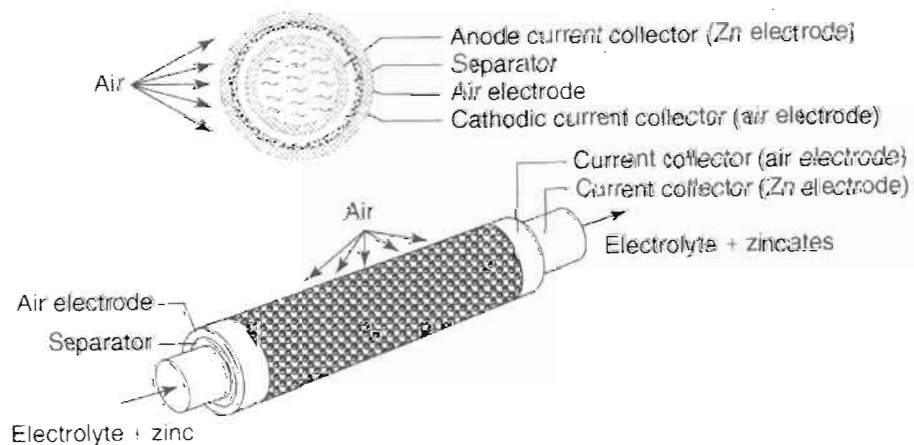
Figure 11: Schematic of a tubular Zn-air cell (Haas *et al.*, 2003:400).

Unlike the solid porous structure of the planar electrode, zinc-air cells also make use of a zinc powder electrode. Haas *et al.* (2003:399) explain that in these batteries, a fluid paste prepared from zinc powder and electrolyte or zinc slurry is continuously moved past a collector electrode during discharge, thereby oxidising the zinc into zincate. Figure 11 shows a schematic view of a tubular slurry cell.

2.3.3   Electrolyte

Unlike the solid polymer electrolyte used in the proton exchange membrane fuel cell (PEMFC) and the direct methanol fuel cell (DMFC), metal air batteries and fuel cells use water based aqueous solution of acids, neutral salts or bases. According to Beck and Rüetschi (2000:2470) aqueous electrolytes have the advantage of being inexpensive and have a relatively high ionic conductivity.

Cairns (2003:301) explains that the fundamental requirement of a fuel cell electrolyte is invariance, i.e. maintaining a constant composition during fuel cell operation while not entering into the net electrochemical reaction of the fuel cell. Features of an invariant electrolyte should be the following:

- Performance should not decrease over extended operating periods due to changes in the electrolyte.
- No spontaneous chemical reactions should occur between the electrolyte and the fuel, oxidant or products.
- The electrolyte should support complete electrochemical oxidation of the fuel.
- The solubility of the fuel and oxidant in the electrolyte should be limited.
- The electrolyte must possess sufficient electrolytic conductivity.
- The electrolyte should not react with any of the cell components.

Electrolytes of acidic nature are rarely used because of the corrosive activity on both the anode and cathode material. Catalyst of such cells should be very stable in acidic conditions, thus narrowing the range of catalyst that can be used. The most widely

used electrolytes for metal-air cells are alkaline based water solutions of potassium hydroxide (KOH) or sodium hydroxide (NaOH). They offer high ionic conductivity and show low corrosion with respect to the different metal anodes. The use of an aqueous alkaline electrolyte broadens the variety of catalysts that can be used at the air cathode (Worth *et al.*, 2002:6).

The disadvantages of using an alkali hydroxide electrolyte is that it is hygroscopic, meaning that it will absorb and lose water depending on the humidity and that it will react with carbon dioxide in the air to form alkali carbonates (Stu.inonu.edu.tr., 2005). Both the absorption and loss of water will negatively affect the conductivity of the electrolyte, thus reducing the overall performance of the cell.

KOH has a much higher ionic conductivity than NaOH (Figure 12). For this reason, zinc-air cells typically make use of KOH as the electrolyte of choice. Bender *et al.* (1995:2) explains that the potassium hydroxide used in zinc-air cells does not get consumed by the reaction and functions only as an ion conductor.
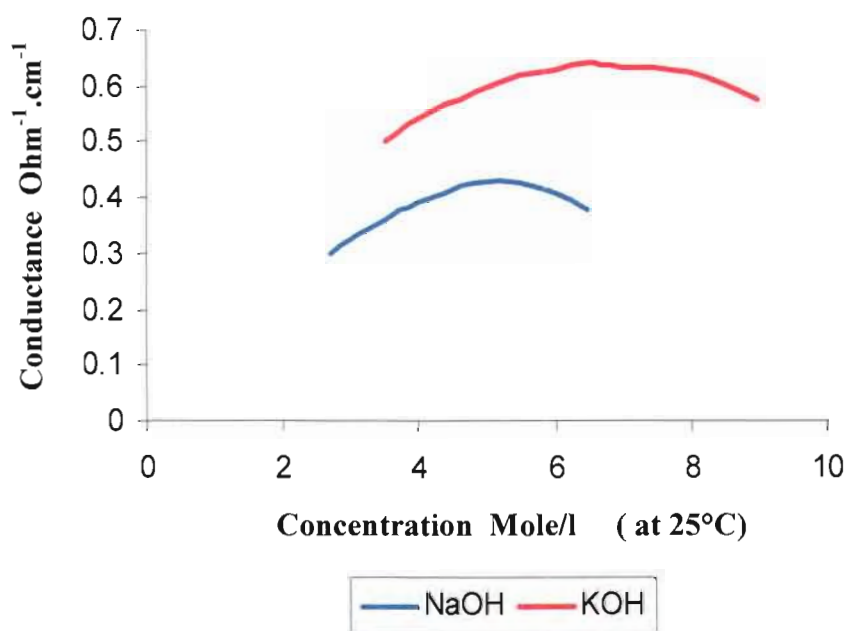
Figure 12: Conductance of KOH and NaOH (Berndt, 1997:208).

As mentioned in section 2.3.1.4, CO_2 reacts with the alkaline electrolyte due to the acidic nature of the CO_2 gas. According to Larminie and Dicks (2003:138) carbonate is formed that affects the cell in the following manner:

- The OH⁻ concentration is reduced, thus reducing the rate of reaction at the anode.
- The viscosity is increased, reducing the diffusion rates, thus lowering the limiting currents and increasing mass transport losses.
- The carbonate salt is less soluble, and will eventually precipitate, blocking the pores and causing damage to the GDE as previously mentioned.
- Oxygen solubility is reduced, increasing the activation losses at the cathode.
- Electrolyte conductivity is reduced, increasing the ohmic losses.
- The performances of the electrode may be degraded.

Bender *et al.* (1995:15) goes on to say that zinc-air cells can be satisfactorily discharged using a carbonated electrolyte. However, extreme carbonation can cause the vapour pressures of the electrolyte to increase, which aggravates water vapour loss in low humidity conditions. Furthermore, crystals of carbonate formed in the cathode structure may impede air access through the GDE as previously mentioned.
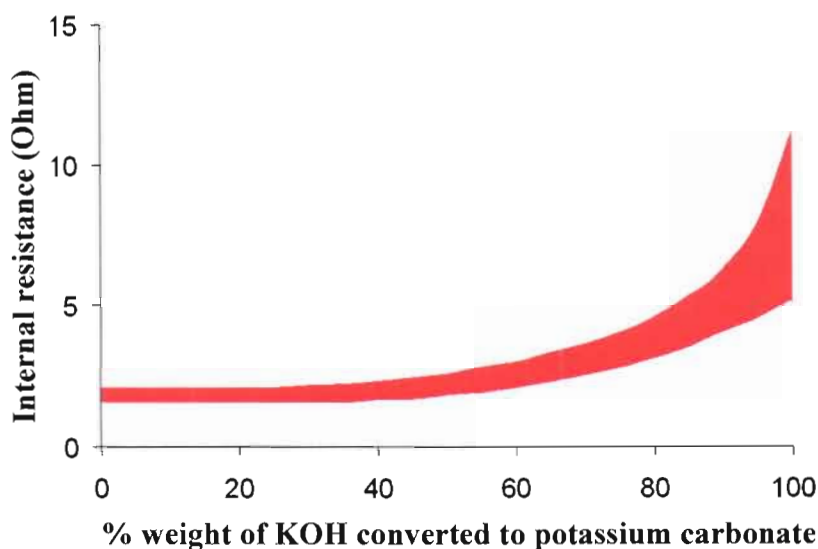
Figure 13: Effect of electrolyte carbonation on internal impedance (Bender *et al.*, 1995:16).

Figure 13 shows to what extent carbonation of the electrolyte affects the internal impedance of a zinc-air cell under test. The performance of the cell only really suffers from carbonation after more than 60 percent weight of KOH has been converted to carbonate. Although the carbonation of the electrolyte has almost no effect on conductivity below 60 percent K_2CO_3, it will have a great effect on the cycle life of the GDE due to blockage in the pores of the electrode.

Other factors that affect the performance and service life of the zinc-air cell are humidity and temperature changes. Inspection of figure 14 reveals that for maximum ion conductivity, a concentration of about 26 percent KOH in aqueous solution will be required. The concentration of KOH determines the relative humidity at which the cell should operate. Substituting this value into figure 15, it can be seen that the relative humidity should be around 60 percent for no water transfer to occur.
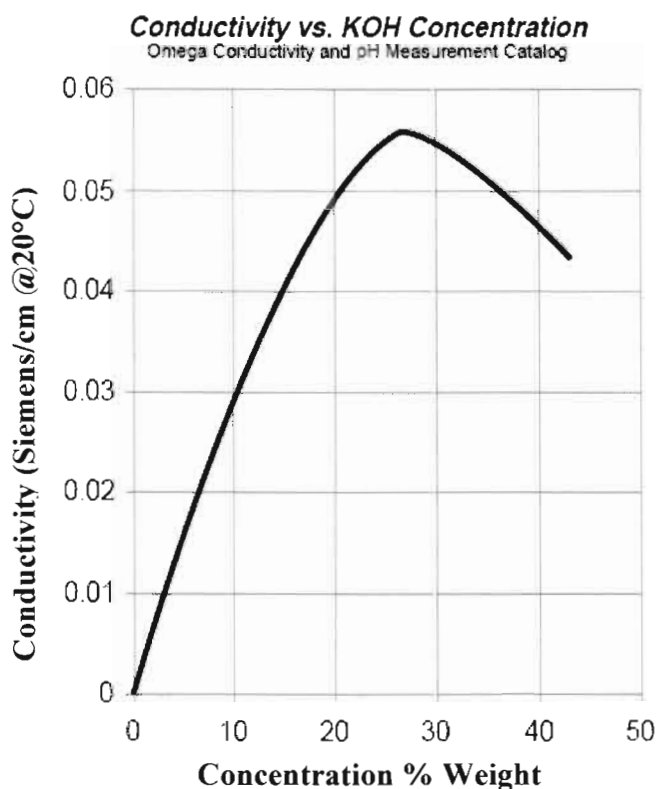
Figure 14: Conductivity curve of KOH (Burger, 2005).
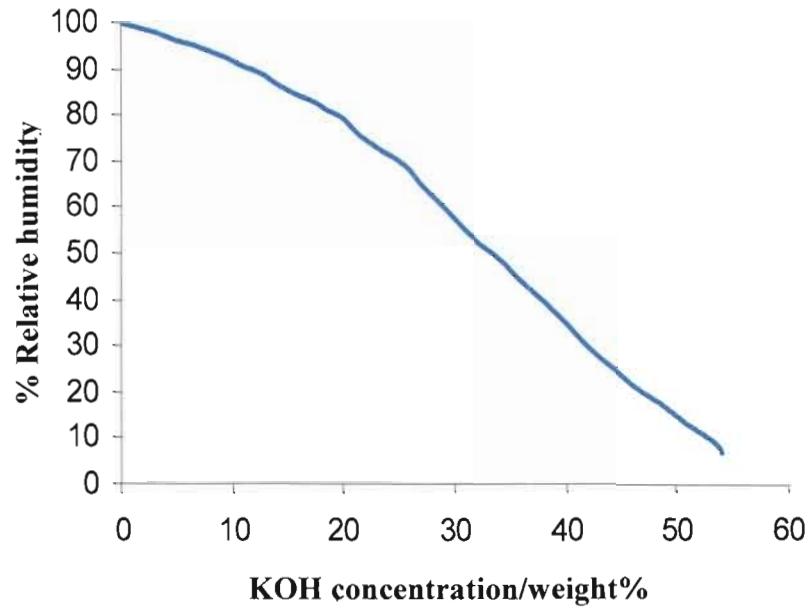
Figure 15: Relative humidity vs. KOH concentration (Berndt, 1997:59).

Bender *et al.* (1995:16) explains that at relative humidities of below 60 percent, water loss occurs which increases the concentration of the electrolyte, eventually drying out the cell to the point where inadequate electrolyte is available to maintain the discharge reactions. At relative humidities of above 60 percent, water gain occurs which dilutes the concentration of the electrolyte, thus reducing the conductivity. Excessive and sustained water gain conditions will also flood the catalyst layer of the GDE, reducing the electrochemical activity and eventually causing the cell to fail.

Temperature affects the cell by decreasing the ionic diffusion capability through the electrolyte, reducing the overall performance of the cell. This is mainly caused by the high concentrations of potassium or sodium hydroxide that are commonly used in these cells. The high concentrations are subject to changes in viscosity, lowering the ion mobility as the temperature drops. The optimum discharge temperature range is between 10 and 40 °C (Bender *et al.*, 1995:13).

2.3.4   Mechanical Separator

Due to the nature of the fuel, zinc-air cells require the addition of some form of mechanical separator material. According to Kiehne (2003:39) separation is required between the two reactions to prevent any contact between the positive and negative electrode which will result in a short circuit, discharging the cell and making it useless.

Jena *et al.* (2001:71) explain that battery separators are porous structures that allow the electrolyte to flow between the different components within a battery. Separators are characterised by their permeability, strength and ability to maximise ionic conductivity.

The first type of separator used in portable batteries were made of wood, but since 1946 these have been replaced by microporous plastics or rubber (Vincent & Scrosati, 1997:150).

Today modern batteries use thin plastic sheets that provide more than 80 percent open volume or porosity (Kiehne, 2003:39). They are usually microporous plastics of either polyethylene or polypropylene.

Dewi *et al.* (2003:149) noted that developments of materials used as separators in metal-air batteries have been very limited, although more novel electrochemical processes are being developed. Commonly used separators are porous membranes such as polypropylene membranes such as Celgard® with a porosity of 10-20 μm.

Companies that manufacture and supply some of these separators include; Advanced Membrane Systems (AMS), Celgard® and DSM.

The features of a good separator can be summarised by the following:
- High porosity to ensure low electrical resistance (Vincent & Scrosati, 1997:150).

- Small pore diameter to achieve good separation (Vincent & Scrosati, 1997:150).
- Good insulation to prevent conduction between plates (Smith, 1980:15).
- Resistance to oxidation and stability in highly concentrated acids (Vincent & Scrosati, 1997:150) and alkalies.
- Absence of harmful impurities (Smith, 1980:16).
- Mechanically weak separators could tear or split, resulting in an internal short circuit (Smith, 1980:16).

2.4 Performance characteristics

The following sections will cover the performance characteristics of the zinc-air cell and the various conditions that effect the operation and performance of such a cell.

2.4.1 Thermodynamic Potential

The theoretical value of the open circuit voltage of the zinc-air cell can be calculated by making use of Gibb's free energy (Equation 2.3). Gibb's free energy describes the maximum amount of chemical energy that can be converted into electrical energy and vice versa (Kiehne, 2003:5). In other words, this is the energy that is available to do external work, ignoring any work done by changes in pressure and/or volume within the cell.

Enthalpy is the Gibb's free energy plus the energy connected with the entropy. The relationship between the three parameters is shown by the following equations:

$$\Delta G = \Delta H - T.\Delta S \quad \text{or} \quad \Delta H - \Delta G = T.\Delta S \quad (2.3)$$

where $T \equiv$ Absolute temperature in K

$G \equiv$ Gibbs free energy in J

$S \equiv$ Entropy in $J.K^{-1}$

The change in Gibb's free energy, ΔG_f, is the energy released by the reaction within the zinc-air cell. This change is the difference between the Gibb's free energy of products and the Gibb's free energy of the input reactions:

$$\Delta G_f = G_f \text{ of products} - G_f \text{ of reactants} \qquad (2.4)$$

For the purpose of the calculations, quantities are considered in their per mole form and are indicated with a " $^-$ " sign over the lower case letter g_f, for example $\bar{g}_f$ is equal to the Gibb's free energy of one mole of a substance. The molar mass of zinc = 65,39 amu, thus, one gram mole of zinc = 65,39 g.

One mole of any substance always has the same number of molecules; this number is called Avogadro's number, represented by the character N, and is equal to $6,022 \times 10^{23}$. Since the charge on one electron is $1,602 \times 10^{-19}$ C, Faraday's constant, F can be calculated with the following equation:

$$F = N \times e \qquad (2.5)$$
$$F = 6,022 \times 10^{23} \times 1,602 \times 10^{-19}$$
$$F = 96485 \text{ C}$$

i.e. one Faraday is the charge carried by one mole of electrons.

The overall reaction of the zinc-air cell is:

$$Zn + \tfrac{1}{2} O_2 \rightarrow ZnO$$
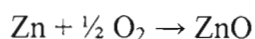
The Gibb's free energy for the zinc reaction at standard conditions at 25 °C is $-318,3$ kJ.mol^{-1}.

The zinc-air cell releases two electrons for every molecule of zinc used, thus for every mole of zinc used, $2N$ electrons pass through the external circuit. If e is the charge on one electron, then the charge that flows throughout the external circuit is:

$$-2N \text{ x } e = -2.F \text{ C} \tag{2.6}$$

If E is the voltage of the zinc-air fuel cell then the electrical work done moving this charge through the external circuit is:

$$\text{Electrical work done } = \text{charge x voltage} \tag{2.7}$$

$$= -2 \text{ F.E J}$$

When the reactants and products of the cell reaction are in their standard states and the system is reversible and has no losses, then the electrical work done is equal to the Gibb's free energy, thus:

$$\Delta \bar{g} = -2F\Delta E^0 \tag{2.8}$$

$$\Delta E^0 = \frac{-\Delta \bar{g}_f}{2F} \tag{2.9}$$

Substituting the values given and obtained above in equation (2.9) yields the electromotive force (EMF at 25°C and 1 atom) or reversible open circuit voltage of the zinc-air cell.

$$E^0 = \frac{-(-318,3 \times 10^3)}{2 \times 96485}$$

$$E^0 = 1,65 \text{ V}$$

The practical open circuit voltage of a zinc-air cell is usually in the region of 1,4 V.

This is lower than the theoretical thermodynamic reversible potential of 1,65 V. The reasons for this and other voltage losses which will be explained in more detail in section 2.4.3.

2.4.2 Energy potential of Zinc

Zinc-air cells have one of the highest energy and volumetric energy densities of all battery and fuel cell systems as will be discussed in section 2.7. This is due to the fact that zinc-air cells have only one of its reactant components within the cell. This means that only the zinc component determines the energy density of the cell. The energy density of one kilogram of zinc can be calculated as follows: First determine the number of moles per kilogram zinc according to the following calculation:

$$\text{Moles}_{Kg} = \frac{1000}{\text{Zinc}_{Atomicmass}} \tag{2.10}$$

$$= \frac{1000}{65,39\text{amu}}$$

$$= 15,293 \text{ mole.Kg}^{-1}$$

By applying Faraday's Law, which states that the charge involved in an electrochemical reaction is equal to the number of moles of the reactant reacting and the number of electrons required for the reaction. Thus the charge involved is:

$$Q = zmF \tag{2.11}$$

Where $z \equiv$ number of electrons

$m \equiv$ number of mole.Kg^{-1}

$F \equiv$ Faraday's constant ($F = 96\,500$ coulombs.mole^{-1})

32

Substituting equation (2.11) with the relevant numbers for the zinc-air reaction we get the charge involved to be:

$$Q = 2e \times 15{,}293 \text{ mole.Kg}^{-1} \times 96\,500 \text{ coulombs.mole}^{-1}$$

$$= 2\,951\,549 \text{ C.Kg}^{-1}$$

Converting the charge per second to ampere hour we get theoretical energy of one kilogram of zinc:

$$Q \rightarrow \text{Ah}$$

$$\text{Zn/Kg} = 819{,}9 \text{ Ah}$$

The specific power density of one kilogram zinc can now be calculated using the formula:

$$P = V_{theoretical} \times I_{theoretical} \qquad\qquad (2.10)$$

$$= 1{,}65 \text{ V} \times 819{,}9 \text{ Ah.Kg}^{-1}$$

$$= 1352{,}835 \text{ Wh.Kg}^{-1}$$

Some researchers suggest that that the true specific power of the zinc air cell should be calculated using the atomic mass of the discharged species zinc-oxide and not just the zinc. The atomic mass of one mole zinc-oxide is:

$$\text{Atomic mass ZnO} = Zn_{weight} + O_{weight}$$

$$= 65{,}39 + 16$$

$$= 81{,}39 \text{ amu}$$

33

Calculating the theoretical specific power using the discharged product results in about 1087 kWh.Kg^{-1}. This shows a 20 percent difference in the theoretical power density when using the discharge product zinc-oxide.

It should be noted that this is only the theoretical energy of the zinc by weight. These values will drop considerably when the weight of additional components such as the GDE, cell housing, electrolyte etc. gets worked into the equation.

2.4.3   Polarization losses

Vincent and Scrosati (1997:58) explain that a typical cell polarization curve consists of three regions. The first region undergoes a rapid fall in cell voltage at low current drains due to electrode polarization overvoltage (Defined as the voltage over and above the voltage predicted from standard tables of reduction potentials that must be applied before an electrochemical reaction occurs at the expected rate). In the second, almost linear region, the internal resistance of the cell components causes further voltage loss (*iR* polarization). In the third region, at relatively high current drains, the *iR* polarization is combined with further electrode polarization caused by the depletion of electroactive materials at the electrode surface. The three regions are indicated in figure 16.

Scott (2004:1208) explains that there are four loss mechanisms within a fuel cell, they are:
- Reactant crossover and internal current losses,
- Activation losses,
- Ohmic losses, and
- gas diffusion losses.

The losses within a zinc-air cell can now be understood using the data and information Scott (2004) used to define the losses within a solid polymer electrolyte fuel cell. Figure 16 represents the V-I curve of an 80 Ah zinc-air cell under test. A full description of the experiment can be found in **Annexure A.**
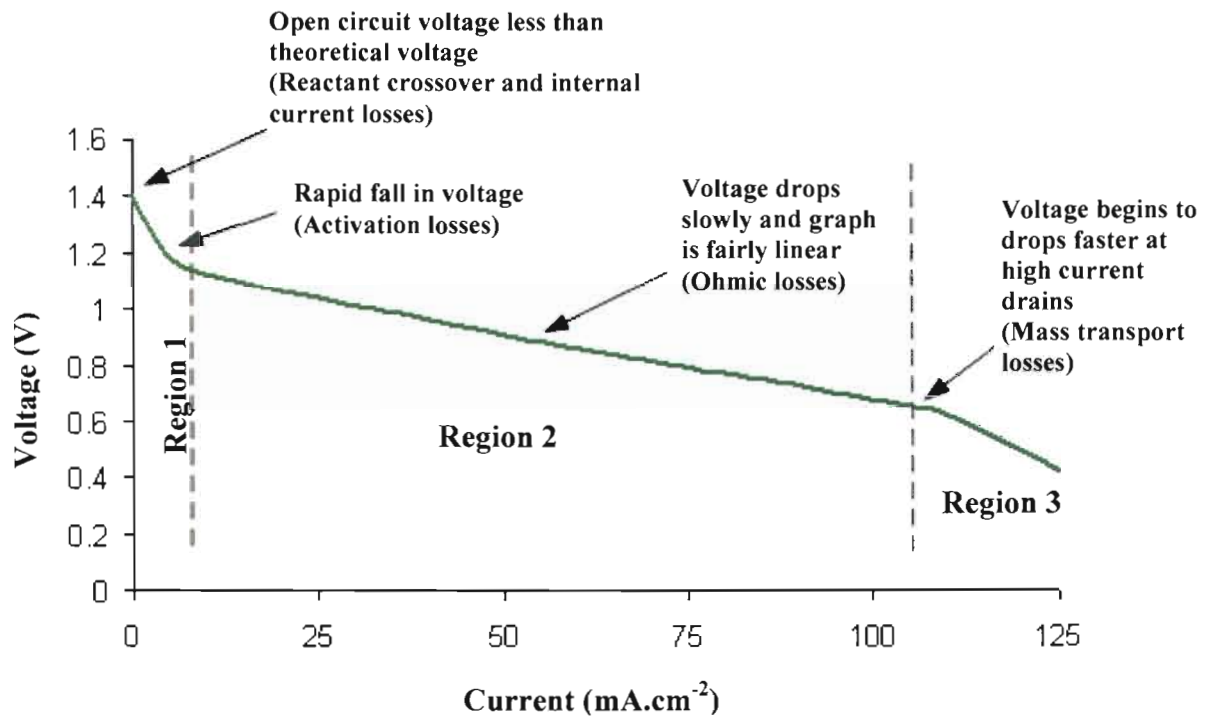
Figure 16: Voltage-current polarization curve (See Annexure A).

2.4.3.1 Reactant crossover and internal current losses

Reactant crossover and internal current losses are to blame for the difference between the thermodynamically expected voltage of 1,65 V and the open circuit voltage of about 1,4 V. There are two reasons for this: (i) While the electrolyte must be a good ion conductor within a zinc-air cell, it must be an excellent electron insulator. Since the electrolyte can not be perfect, there will always be some trace of current flow through the electrolyte which will result in a voltage drop. (ii) There will also be some trace of reactant migration through the electrolyte producing useless heat.

2.4.3.2 Activation losses

Activation losses (region 1; at low current densities) occur when the initial current begins to flow, causing a steep decline in voltage before the curve flattens out. The reason for this is that electrochemical reactions naturally proceed rather slowly (particularly at the cathode) and require activation by way of an increase voltage drop that "pulls" the charged particles across the electrode-electrolyte double layer interface. The voltage will usually fall to about 1,2 V, allowing the current to flow more rapidly.

2.4.3.3 Ohmic losses

Ohmic losses (region 2; at mid current densities) are losses that are connected with the current flow through the components of the power source. The ohmic losses originate in the electrolyte, the gas electrodes, the connection electrodes and any other material through which both electronic and ionic currents must flow inside the cell.

2.4.3.4 Gas diffusion losses

Gas diffusion losses (region 3; at high current densities) as well as the consumption of the solid electroactive material zinc, in the zinc-air cell, are responsible for the voltage loss in region 3. As the current increases there comes a point when the reactant gas and zinc electrode are being consumed at such a rate that starvation of the electrolyte-electrode interfaces occur. Usually, suffocation is most severe because the O_2 is already diluted by the air's N_2. N_2 is also responsible for reducing the rate at which O_2 diffuses through the pores of the gas diffusion electrode, blocking the pores, thus preventing or slowing the diffusion of O_2. At the anode, zinc is oxidized at such a rate that a barrier of zinc-oxide forms around the electrode, increasing the internal resistance and decreasing the area of the zinc. The point at which these constraints begin to limit efficiency is usually near the point of maximum power which will seldom be reached in practical cell operation.

2.5.4   Discharge characteristics

The discharge curve or voltage profile is the relationship of a cell's voltage to the length of time it has been discharging. The two profiles that exist are: (i) The flat discharge curve and (ii) the sloping discharge curve. Batteries with sloping voltage profiles provide power that is adequate for applications such as flash lights, flash cameras and portable radios. Batteries with a flat voltage profile have a relatively constant output voltage for more than two thirds of its discharge cycle with a sharp drop in voltage near the end of its cycle. Applications that require a steady operating voltage commonly use a battery of this profile (Site.greenbatteries.com/, 2006). Figure 17 shows a graphic representation of these two profiles.

— · — · — Sloping discharge curve ———— Flat discharge curve
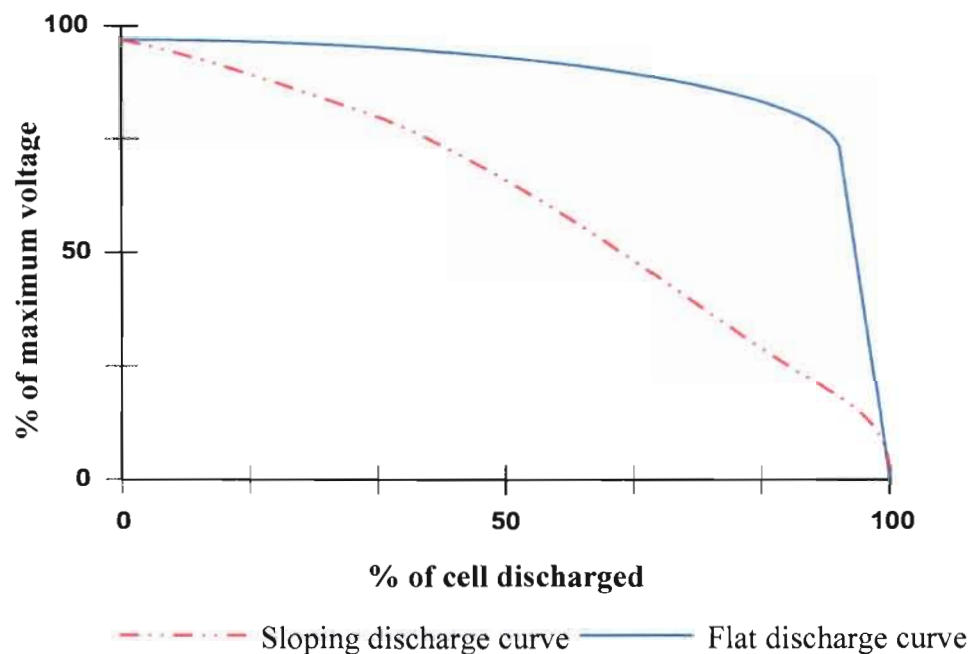
Figure 17: Sloping discharge and flat discharge profiles (Travis, 1997:17).

An experiment was carried out to determine the profile that represents the discharge curve of the zinc-air cell. A full description of this experiment is in **Annexure B**. The result of the experiment is shown in figure 18. It shows that the discharge curve of a zinc-air cell has a flat voltage profile.

The disadvantage of using a battery with a flat voltage profile is that it will need to be replaced almost immediately after a noticeable drop in voltage occurs. If this is not done right away the battery will quickly cease to provide any useful energy (Travis, 1997:17).
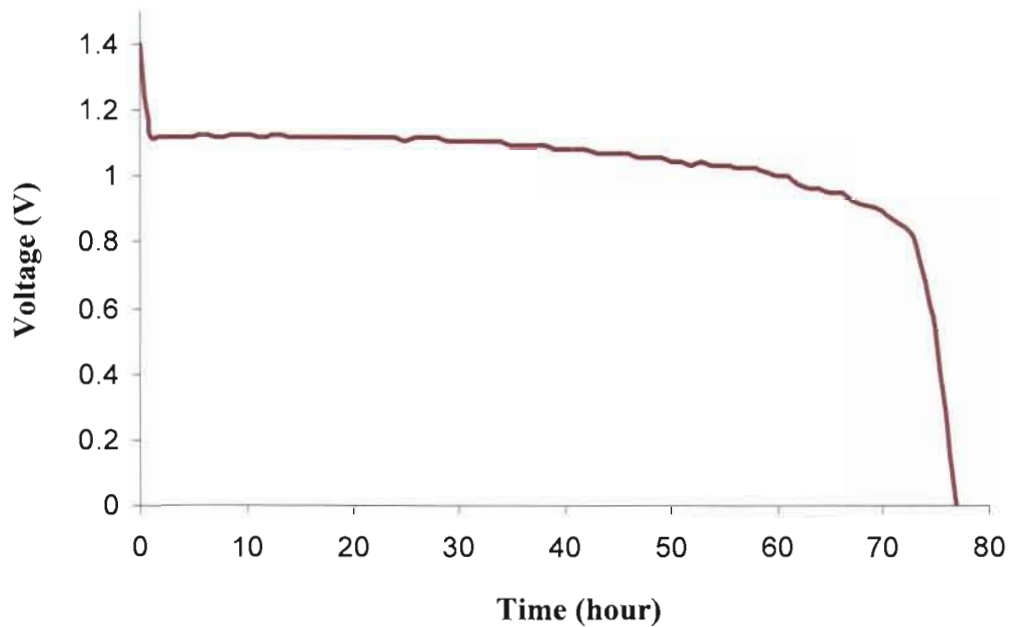
Figure 18: Discharge curve of an 80 Ah zinc-air cell (See Annexure B).

2.5.5 Environmental effect on cell performance

As explained in section 2.3.3, changes in both temperature and humidity greatly affect the efficiency of the electrolyte and thus the performance of the zinc-air cell.

Figure 19 shows the intermitted discharge of a zinc air battery at 30, 60 and 90 percent relative humidity. At 60 percent relative humidity (RH), the least amount of moisture transfer occurs and the cell delivers the maximum service (Bender *et al.,* 1995:18).
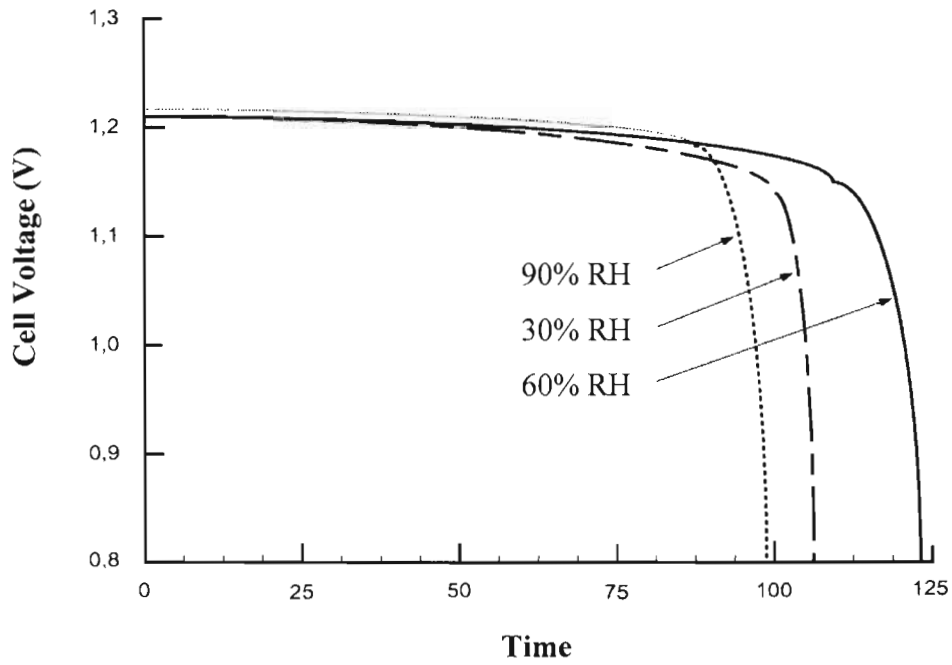
Figure 19: Discharge characteristics at various levels of RH (Bender *et al.*, 1995:18).
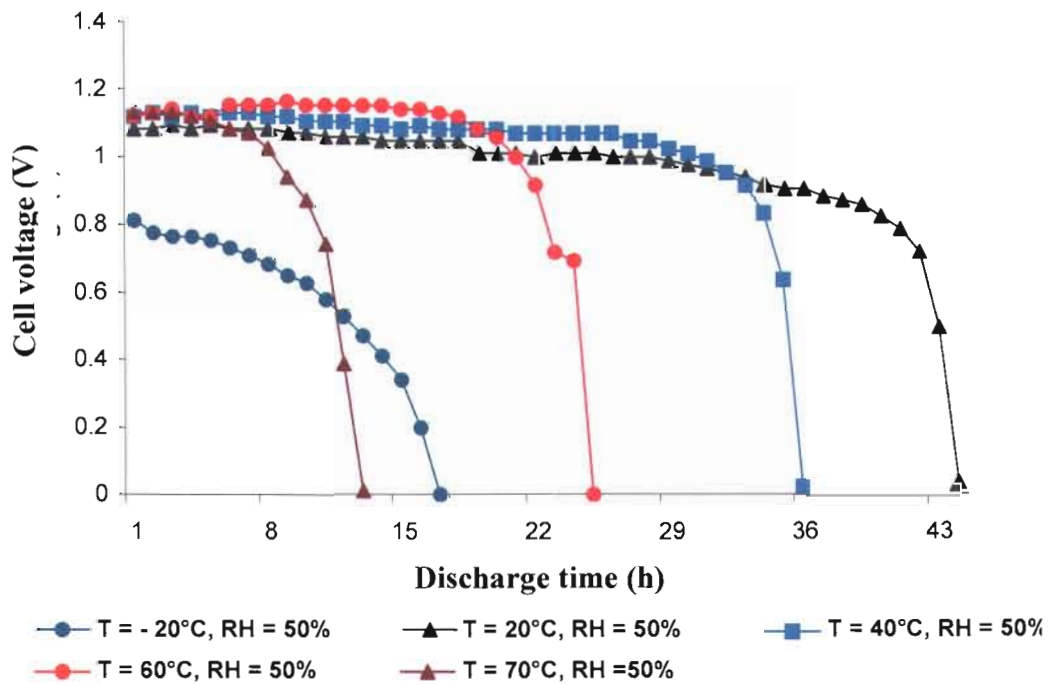
Figure 20: Discharge characteristics at various temperatures (See Annexure C).

Section 2.3.3 also mentions that temperature affects the cell by decreasing the ionic diffusion capability through the electrolyte. Figure 20 shows the effect of temperature variation on the discharge performance of an 80 Ah zinc-air cell. The cell was discharged at a constant two amperes until fully discharged. Bender *et al.* (1995:13) also mention that the operating voltage varies with temperature. This can also be seen in the graph of figure 20. A full description of the experiment can be found in **Annexure C**.

Bender *et al.* (1995:13) also explains that at low discharge rates and moderate temperatures, the effect of temperature is minimal, thus, when selecting a zinc-air system that must perform at low temperatures, it is important to consider the current density in order to prevent failure due to diffusion limitations.

2.6 Safety and environment

Naimer *et al.* (2002:1) explain that, in addition to its outstanding performance, zinc-air technology has two additional features, which are:

- Safety: The cell is inherently safe in storage, transportation, utilization and disposal. Unlike other battery technologies, zinc-air cells offer lower danger of fire, explosion or personnel exposure to hazardous materials. Thermal runaway or combustion that may occur due to a short circuit, either internal or external, is prevented by the current being limited by the oxygen permeability of the air electrode. In addition, exposure of the active anodic material to the environment poses no fire hazards.
- Environment: Hazardous elements such as mercury, lead or cadmium that are normally used in other battery technologies are not present in zinc-air cells. Zinc-air cells are safe enough to be disposed of with everyday household trash.

Although the cell itself is not harmful to the environment and reasonably safe, KOH on its own is hazardous to the human body. Potential health effects of KOH on the human body (Iowa State University, 2002) is as follows:

- Eye: Causes severe eye burns. May cause irreversible eye injury. Contact may cause ulceration of the conjunctiva and cornea. Eye damage may be delayed.
- Skin: Causes skin burns. May cause deep, penetrating ulcers of the skin.
- Ingestion: Harmful if swallowed. May cause circulatory system failure. May cause perforation of the digestive tract. Causes severe digestive tract burns with abdominal pain, vomiting, and possible death.
- Inhalation: Harmful if inhaled. Irritation may lead to chemical pneumonitis and pulmonary edema. Causes severe irritation of upper respiratory tract with coughing, burns, breathing difficulty, and possible coma.
- Chronic: Prolonged or repeated skin contact may cause dermatitis. Prolonged or repeated eye contact may cause conjunctivitis

2.7 Potential

Beck and Rüetschi (2000:2468) termed the factors that determine the success of a battery system as the "three E criteria". They are:
- Energy (high energy content with respect to unit weight and volume)
- Economics (low manufacturing cost, low maintenance during use, long service life)
- Environment (free of toxic materials, safe, low energy consumption during manufacture and use, long service life, high reliability, easy to recycle)

Zinc-air cells comply well with the criteria set by Beck and Rüetschi (2000). As a source of energy, zinc-air cells have some of the highest specific and volumetric energy densities of all battery and fuel cell systems as shown by figures 21 and 22. On the topic of economics, zinc-air cells use cheap materials and are easy to manufacture. The major advantage that zinc-air cells have over other fuel cell technologies is that zinc-air cells do not require any noble metals, reducing the overall price of such a system. Zinc, as the metal of choice, is also one of the most

41

abundant base metals on earth and also the cheapest. Zinc-air cells are also environmentally friendly and safe as described in the previous section.

All of this emphasises the need to increase the research and development in zinc-air cell technology.
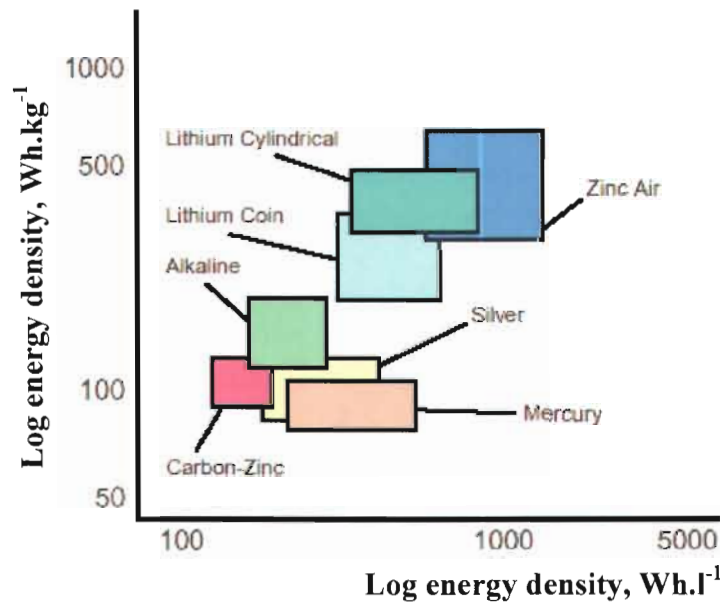
Figure 21: Energy densities of various primary battery systems (Brodd, 1999:21).
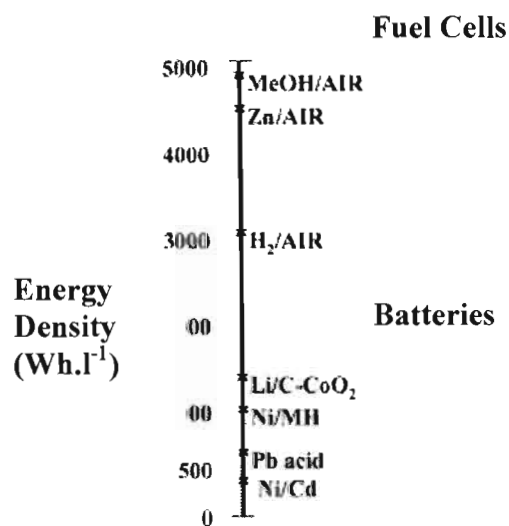
Figure 22: Theoretical energy densities of electrochemical cells (Dyer, 2002:32).

2.8 Summary

This chapter introduced the reader to the technology of the zinc-air cell. It discussed the electrochemical operation, the electrical characteristics of the cell under various conditions and the different components within a zinc-air cell.

The practical design and development of a zinc-air fuel cell are discussed in the next chapter (Chapter 3) along with a definition for the particular fuel cell. Auxiliary systems required for the operation of the cell are also described in chapter 3.

Chapter 3   Fuel cell system design

3.1   Introduction

In the previous chapter, the reader was introduced to the technology of the zinc-air cell, its different components and the variables that affect its performance. This chapter deals with the design and development of a zinc-air fuel cell system and the problems that were encountered. The system is divided into separate sections, the sections being the zinc-air cell, the fuelling and removal mechanism, the electrolyte circulation system and the control unit. The design concept within this dissertation for the system under discussion has, as far as it could be established, not been attempted before.

Due to the confusion that surrounds the terminology of the zinc-air cell and its technology, a clear definition must first be formulated before any design can be established for the zinc-air fuel cell. Formulation of this definition will be covered in the following section.

3.2   Defining the zinc-air fuel cell

In the literature, reference to zinc-air technology is made as either, a zinc-air battery, a zinc-air fuel cell or when unsure, a zinc-air cell. Vincent and Scrosati (1997:3) explain that a power source, in which one of the active reactants are in the gaseous state, must be termed a hybrid cell. This raises the question: What is a zinc-air fuel cell and can it be classified as a fuel cell? To establish a clear definition for the zinc-air fuel cell, a comparison with other fuel cells is needed to find the common factors that classify them as fuel cells.

A definition for the zinc-air fuel cell can be found by examining the two most popular fuel cells currently under development. These are the PEMFC and the DMFC. The most common factors between both these and the zinc-air cell are that

they all are electrochemical cells that convert chemical energy into electrical energy and that they all use oxygen from the atmosphere as the oxidant.

The major difference's between the three cells is the type of fuel used and the state in which it is. Thus the type and state of the fuel is not a classifying characteristic of a fuel cell. PEMFC uses gaseous hydrogen and the DMFC a concentration of liquid methanol whereas the zinc-air cell uses zinc in its solid state.

The obvious difference between PEMFC, DMFC and zinc-air cells is in the way the fuel is stored. Both the PEMFC and DMFC store fuel external to the cell housing. The cell housing only acts as an area for the reactions to take place. Similarly a zinc-air cell can only be classified as zinc-air fuel cell when the zinc is stored outside the cell housing. The advantage of this is that unlike a battery, fuel cells can never "run flat" as long as there is a constant supply of fuel.

Colborn and Smedley (2001:577) confirm this by explaining that a zinc-air fuel cell differs from a zinc-air battery because the cell is refuelled with the addition of zinc metal to a fully assembled unit; the unit is neither discarded like a primary battery nor disassembled or slowly recharged like a secondary battery.

A zinc-air fuel cell can thus be defined as a device that electrochemically converts the chemical energy of a fuel and an oxidant in to electrical energy. The fuel and oxidant are stored outside the cell and transferred into the cell as the reactants get consumed.

3.3   Zinc particle fuel

The particulate zinc fuel that will be used with the design of the zinc-air fuel cell was donated to the Vaal University of Technology for research purposes by Zincor. The zinc purity is 99,99 percent. Figure 23 shows a photograph of the zinc particles.

Figure 23: Zinc particles.

3.4 Zinc-air fuel cell system

In addition to the design of the zinc-air fuel cell itself, other equipment and design requirements are necessary for the fuel cell to operate successfully. Equipment such as external pumps and tanks for storage of both the zinc, discharged zinc and electrolyte are required as well as an electronic control unit for monitoring the potential of the stack and controlling the zinc feed to the cell to maintain a predetermined discharged voltage. Figure 24 shows a block diagram of a complete zinc-air fuel cell system.
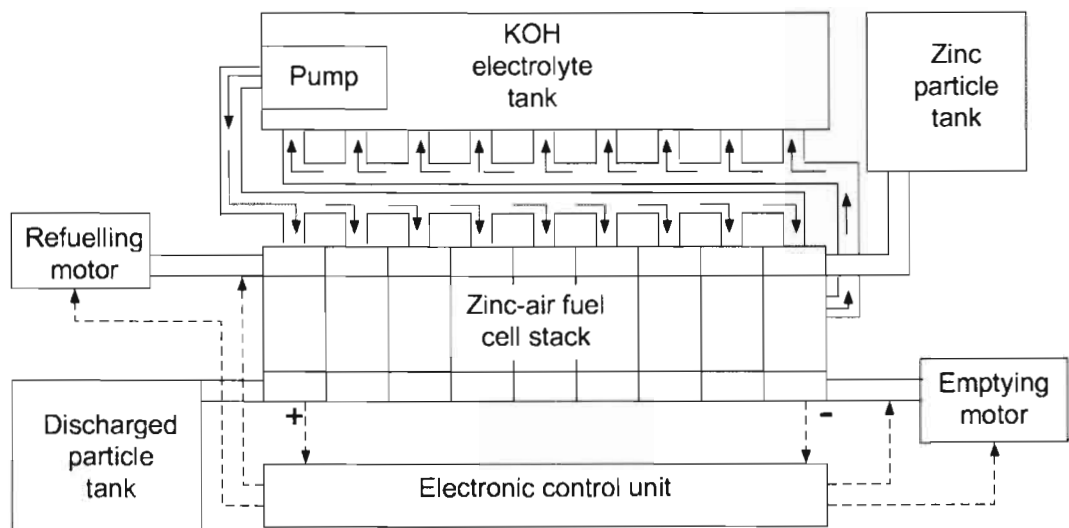
Figure 24: Block diagram of zinc-air fuel cell system.

46

3.4.1 Cell design

The design of a zinc-air fuel cell revolves around the GDE. The power capability of a zinc-air fuel cell is directly proportional to the size or area of the GDE. The zinc-air fuel cell was designed using the existing electrically rechargeable zinc-air batteries that were supplied to the Vaal University of Technology for research purposes by Kumba Resources. These batteries have a prismatic shape with a dual GDE. The active area of one of these GDE's is 90 mm by 120 mm giving a total active area of $1,08 \times 10^4$ mm^2 for a single GDE. Making use of a second GDE doubles the active area of a cell, increasing the power density of the cell. Figure 25 shows a photograph of the GDE that was used in the design and experimentation of the zinc-air fuel cell.
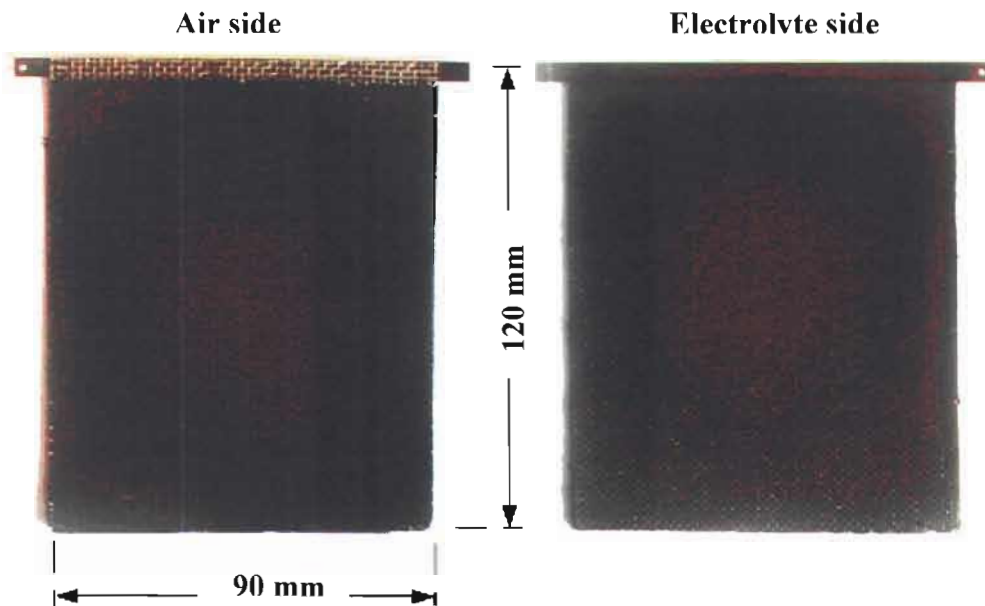
Figure 25: Individual sides of a GDE.

For the zinc-air fuel cell to operate at maximum potential, efficient air access is necessary, for which sufficient provision should be made when stacking individual cells together. This can either be done by placing porous spacers between the cells or, in the case of the cells that were donated to the University, incorporating spacers in the design of the mould. Putt and Woodruff (1993:1085) explain that the

47

thickness of the spacer depends on the lateral dimensions of the cell and current density required by the application. If the spacer is too thin, interior portions of the cathode will become oxygen starved, while if it is too thick the volume of the stack will be unnecessarily large.

The zinc-air fuel cell was designed and developed to operate at about 15 percent of its maximum power capability, to avoid the drastic efficiency losses of zinc fuel at high discharge rates. Thus the spacing was kept to a minimum, decreasing the total volume of the system. The space between the individual cells in the development of the zinc-air fuel cell was determined by the fuelling mechanisms discussed in section 3.4.2.

A form of separator material was required between the GDE and the zinc electrode to prevent short circuiting between the two electrodes. The size of the separator material had to be the same as the active area of the GDE, which was calculated to be $1,08 \times 10^4$ mm^2. The separator used was a microporous polypropylene membrane coated with a wetting agent for additional absorption to increase electrolyte porosity, called Celgard® 3400.
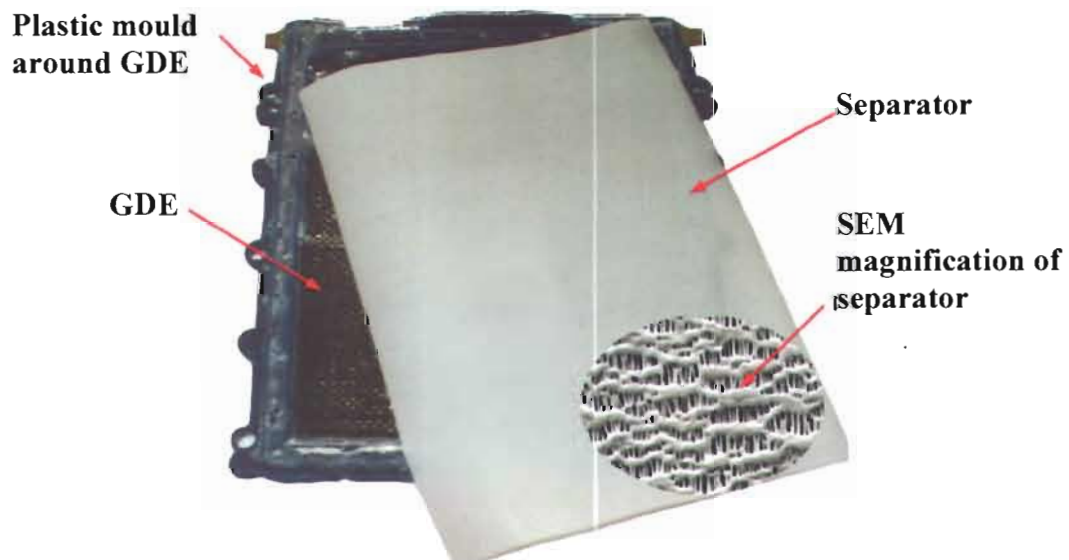
Figure 26: Separator material and moulded GDE.

The separator material was placed and fixed to the moulded GDE as shown in figure 26. This prevents the zinc and its discharged specimen from reaching the GDE while being totally porous to the electrolyte, ensuring maximum flow as well as ionic conductivity between the cathode and anode.

Due to the particulate nature of the zinc, a conductive metal was needed to act as a current collecting electrode allowing current to flow. The metal had to be the same size as the GDE, corrosion resistant and non-reactive. A nickel metal grid was used for this purpose. A grid was used instead of a solid plate as this allowed electrolyte diffusion and prevented concentration unbalances within the cell. Figure 27 shows the nickel grid with metal tab for current collection.
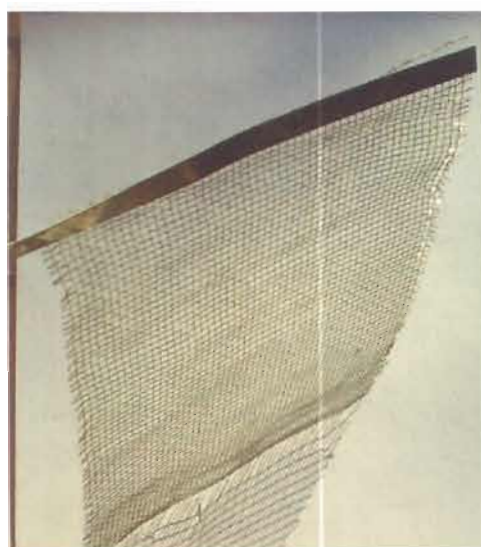
Figure 27: Current collecting grid.

The zinc-air fuel cell made use of a mobile electrolyte system for electrolyte circulation (explained below). This required the addition of an electrolyte input and output system to the cell design. In terms of this design, the electrolyte is pumped in at the bottom of the cell and the overflow at the top is returned to the electrolyte tank for recirculation.

Figure 28 illustrates the two different electrolyte flow inputs that were considered in the design of the fuel cell system. The first, a "concentrated" electrolyte flow, was tested but not implemented due to the following reasons:

- The electrolyte flow pressure opened a void, reducing the overall active area between the GDE and zinc particles.
- The concentrated flow transferred some of the zinc particles through the overflow, reducing the overall energy efficiency and unnecessarily wasting zinc.
- The refuelling process was somewhat ineffective as some of the zinc particles got clogged at the opposite corner of the inflow of the electrolyte.

Concentrated electrolyte flow　　　　Dispersed electrolyte flow
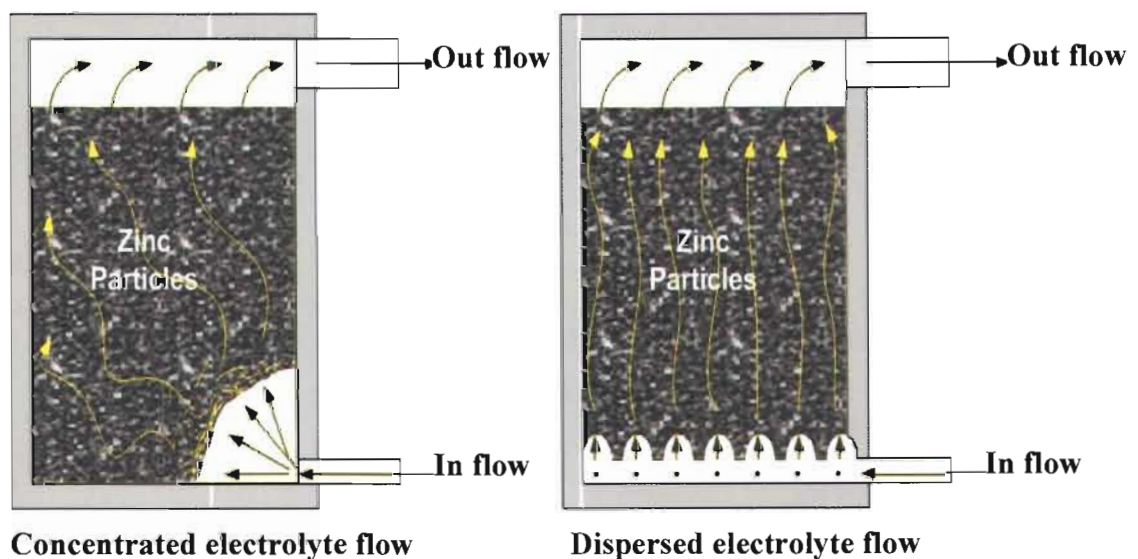
Figure 28: Concentrated electrolyte flow and dispersed electrolyte flow.

The dispersed electrolyte flow avoided the problems associated with the concentrated electrolyte flow by evenly distributing the pressure and flow over the entire width of the cell. Figure 29 shows a photograph of a test carried out on the dispersed electrolyte flow. It shows an even distribution of electrolyte flow from within the electrolyte feeding pipe.

Figure 29: Dispersed electrolyte flow test.

Chakkaravarthy *et al.* (1981:204) say that the zinc electrode within the cell must be completely immersed in the electrolyte or else there will be wasteful corrosion leading to premature discharge. The reason for this being severe oxidation of the zinc metal at the solution-air junction. Therefore, the electrolyte overflow is positioned at such a point that the zinc particles are constantly immersed in the electrolyte.

3.4.2 Fuelling and discharge mechanism

The biggest obstacle in developing a zinc-air fuel cell is in the design of an effective refuelling system. Difficulties arise when designing a suitable refuelling process because the zinc is in a solid state, which makes it almost impossible to circulate through the fuel cell stack as is done in both the methanol and hydrogen fuel cells. Another problem in trying to design a circulating zinc-air fuel cell is that zinc is conductive; this means that even though the stack is made up of a number of cells, they will effectively all be connected to each other.

For the refuelling to be effective, each cell should be refuelled individually from each other without the zinc being connected to each other. The objective of the refuelling system is to have a mechanism that will introduce fresh dry zinc particles to the cell when required. The zinc will then pass through the cell by gravitational

51

forces and be discarded at the bottom of the cell by the same mechanism used for refuelling. Figure 30 shows a simplified illustration of this process.
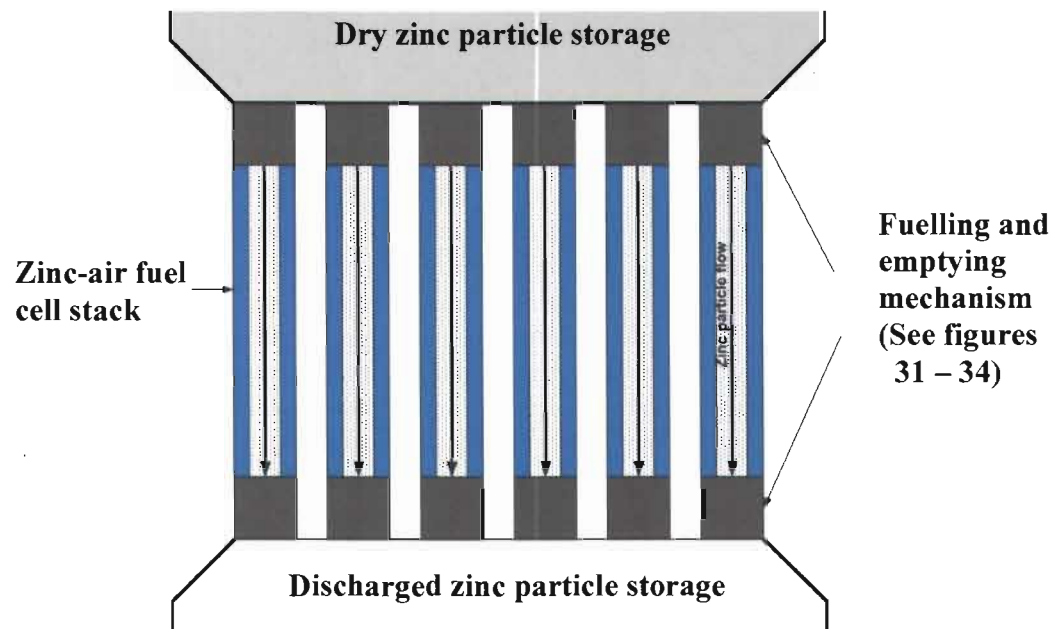
Figure 30: A simplified illustration of the zinc fuelling and discarding process.

The mechanism is based on a rotor with a slot into which the zinc particles can fall. The rotor housing has openings (slits) at the top and bottom. These slits are of the same width and length as the slot within the rotor. Zinc particles fall into the slot at the top of the rotor and drop to the bottom of the cell with each rotation. The same process is repeated below the cell were the discharged zinc is removed from the cell. The design was done on AutoCAD. Figure 31 is an illustration of this designed mechanism.

Due to the aqueous electrolyte, some form of seal had to be incorporated to the discharge mechanism to limit the amount of leaking. This was done by cutting a slot into the blocks and inserting a seal. Sponge-like, compressible seals were used to prevent resistance to rotation. The positions of these seals are indicated in figure 32.
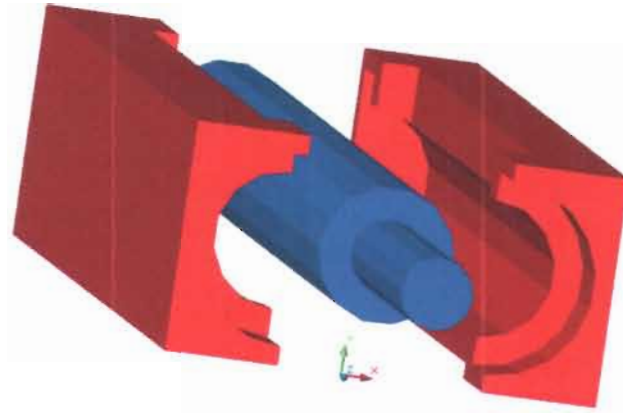
Figure 31: Graphic illustration of the refuelling and discharge mechanism.
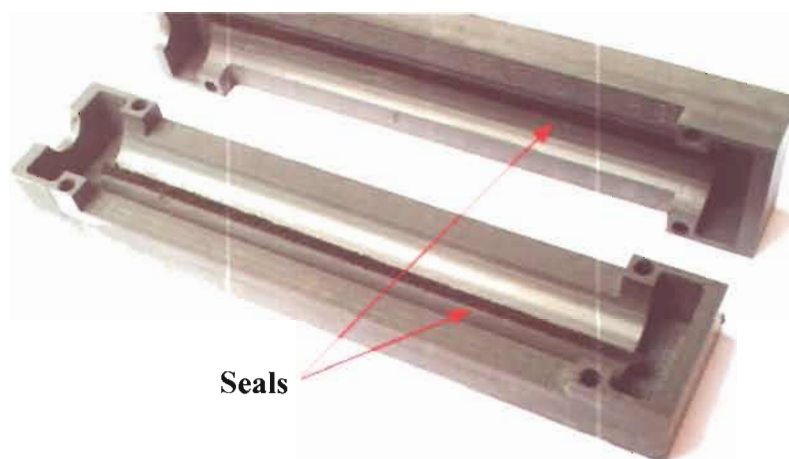
Seals

Figure 32: Location of seals within the rotor housing.

Bearings

Rotor
housing

Rotor

Zinc particle slot
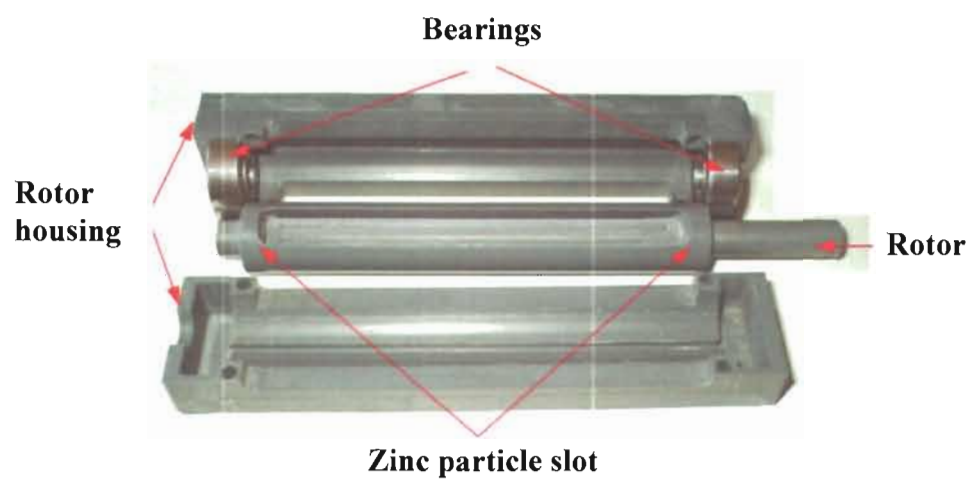
Figure 33: Single mechanism assembly components.

Figure 33 is a photograph of the components within the refuelling and discharge mechanism that was used in the design of the zinc-air fuel cell. The Technology Station at the Vaal University of Technology machined the mechanism out of a polyvinyl chloride (PVC) material.

Rotation is achieved by connecting a gear to the rod which is driven by a chain connected to an electric motor. The electric motor and rotor position is controlled and monitored by an electronic control unit. This unit is discussed in more detail in section 3.4.5. Figure 34 is a photograph of the final mechanism assembly.

Figure 34: Final mechanism assembly.

Figure 35 shows the assembly of the zinc-air fuel cell together with the fuelling and discharge mechanism. The illustration clearly shows the location and sequence of the individual components within the cell assembly. The current collecting grid is positioned in the centre of the cell while the GDE and separator are fixed to the housing of the cell, leaving a void where the zinc particles can be introduced. The fuelling and discharge mechanisms are fixed to the top and bottom of the cell after assembly. Figure 36 shows a photograph of a complete cell assembly with the fuelling and discharge mechanisms.
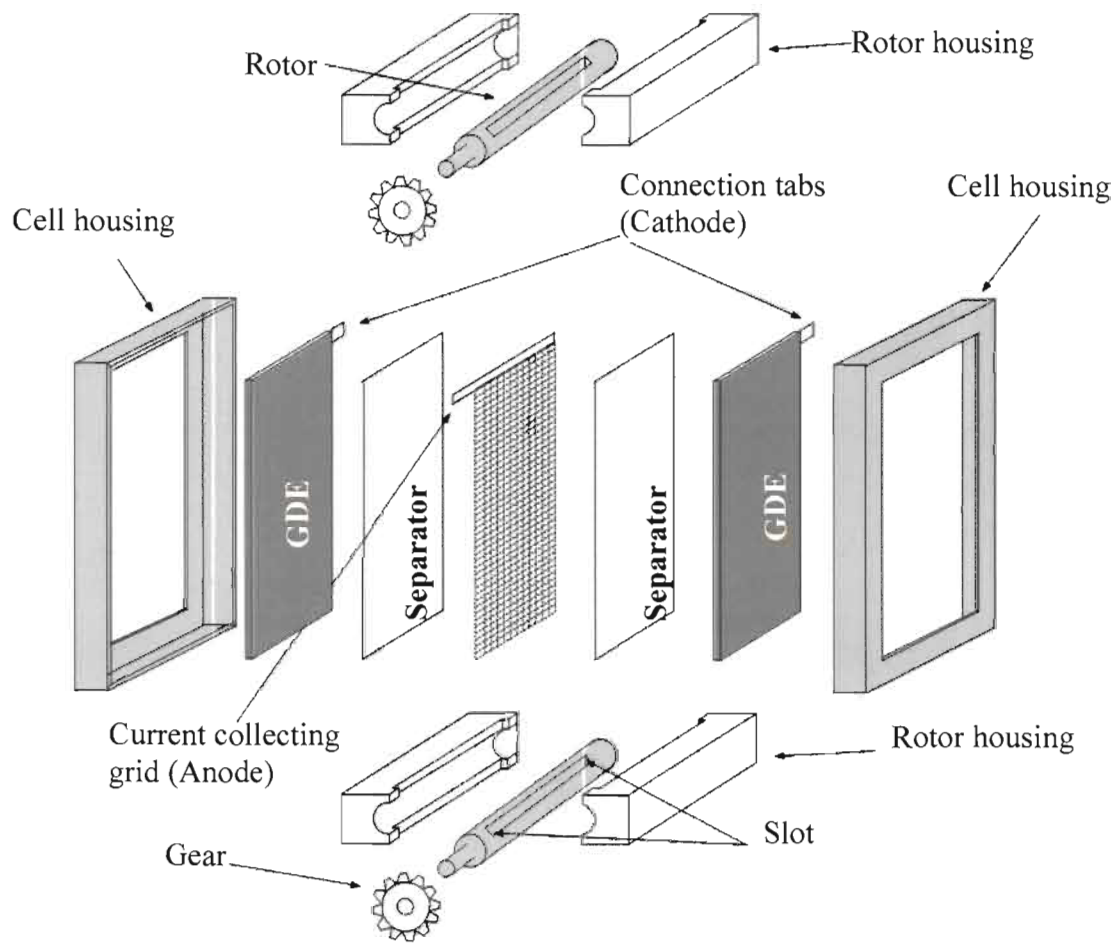
Figure 35: Cell assembly with fuelling and discharge mechanism.

Figure 36: Complete assembled cell with fuelling and discharge mechanism.

3.4.3 Electrolyte circulation system

Two types of designs of electrolyte flow can be used in the design of a zinc-air fuel cell. They are the static electrolyte-type and mobile electrolyte-type. In a mobile electrolyte fuel cell a common supply of electrolyte is pumped and circulated through the fuel cell stack, while in a static electrolyte fuel cell each cell has it's own, separate electrolyte within the stack (Figure 37).
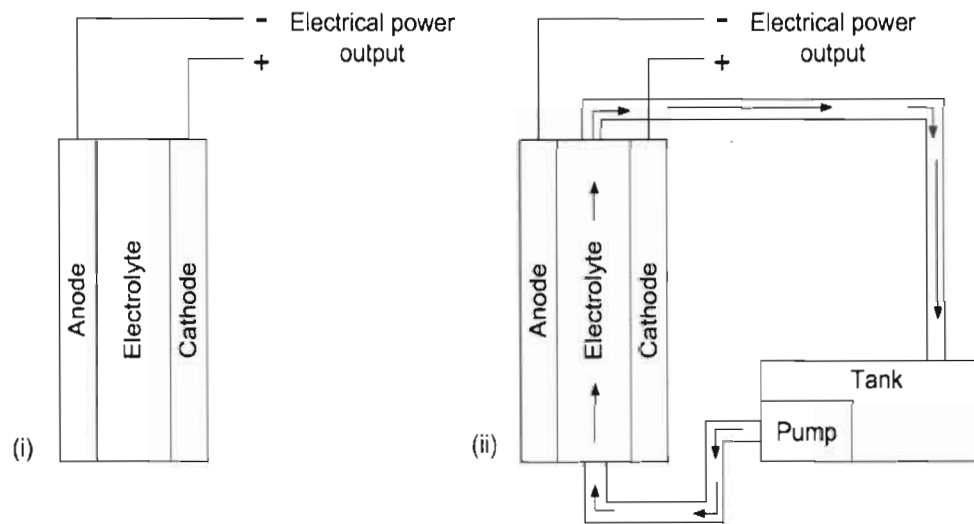
Figure 37: (i) Static electrolyte design and (ii) mobile electrolyte design.

The static electrolyte design was not considered because there are advantages in using a mobile electrolyte-type fuel cell design which can be summarised as follows:

- The circulating electrolyte serves as a cooling system for the fuel cell (Larminie & Dicks, 2003:126).
- The electrolyte is continuously stirred and mixed (Larminie & Dicks, 2003:126).
- Ease of monitoring and controlling the concentration of the electrolyte.
- Ease of replacement of solution, when it has become too diluted with carbon dioxide (Larminie & Dicks, 2003:126).

In addition to the above, and applicable only to zinc-air fuel cells, is that the zinc particles are continuously washed by a flow of re-circulating electrolyte. This circulation removes the reaction product (zincate), which prevents precipitation of the discharged products in the electrode active area. Without this, the cell would quickly become clogged and would not be refuelable (Metallicpower.com, 2004).

Some disadvantages of a mobile electrolyte-type fuel cell are (Larminie & Dicks, 2003:126):

- A suitable pump is needed due to the corrosive properties of the fluid being pumped.
- The extra pipe work increases the possibilities of leaks and due to the low surface tension of the KOH solution fluid could find its way through the smallest of cracks.
- Since the electrolyte is pumped throughout the fuel cell stack, the cells are effectively joined together, creating an internal-short circuit between the cells within the stack.

The mobile electrolyte design consists of a rectangular tank of the same length as that of the fuel cell stack. A submersible pump was fixed into the tank and a common pipe was used which forked into each individual cell, supplying the electrolyte to the cells. On cell overflow, the electrolyte returns to the tank, allowing a constant recirculation of the electrolyte.

3.4.4 Control unit.

Unlike the constant circulation of hydrogen in the PEMFC and methanol in the DMFC, the zinc-air fuel cell is refuelled at intervals at which the voltage reaches a predetermined value. For this reason, some form of electronic monitoring and control is necessary.

The purpose of the electronic monitoring system is to monitor the stack voltage and control the refuelling and emptying of cells when required. This is done by programming the unit with an upper voltage limit which relates to a fully recharged stack and a lower voltage unit which relates to a discharged stack. At these limits, the unit will either start or stop the refuelling and emptying process. Two sensory inputs are also included into the design to determine the position of the rotational rods of both the refuelling and discharge mechanisms. The position of the rotor is important because the cell will suffer extensive leaking if the position is such that the seals are not in full contact with the sides of the rotor. Figure 38 illustrates this process.
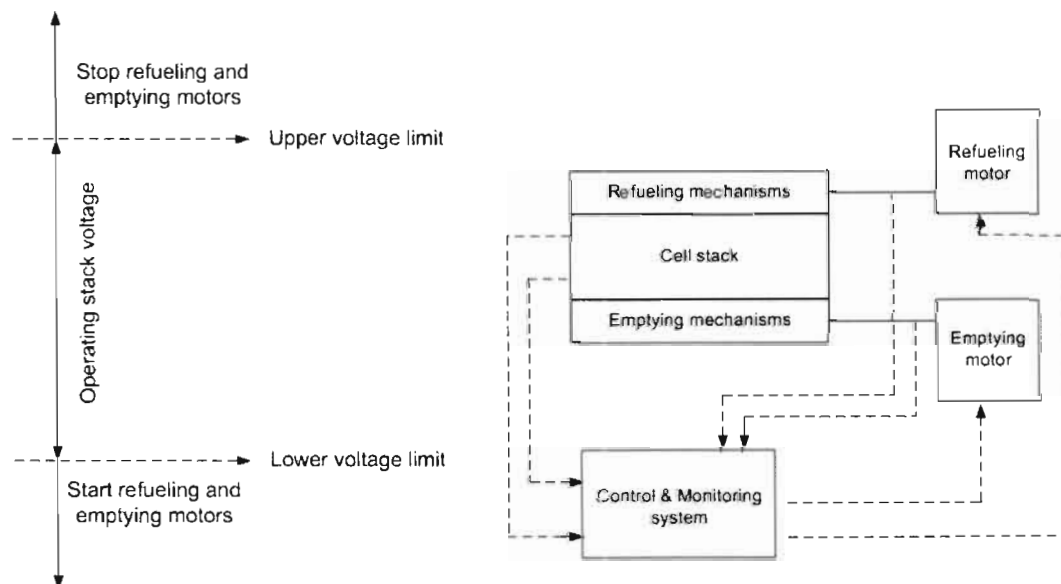
Figure 38: Monitoring and control diagram.

The monitoring and control unit was developed using the PIC16F877 microcontroller from Microchip. The software was written in flow code and used with MPLab to program the software code. Programming hardware such as the In Circuit Debugger (ICD) and the Development Board from Electron was used. A full description of the flow code can be found in **Annexure D**. Figure 39 shows the circuit diagram of the control unit.

Figure 39: Circuit diagram.

Figure 40: Final PCB design.

The test cell was designed using AutoCAD 2002 and machined by the Technology Station that is on campus at the Vaal University of Technology. Some features of the cell are that all the components is easily interchangeable while the temperature of the electrolyte can also be varied through a temperature controller that is connected to the temperature probe and heating element. The electrolyte is also circulated through the cell by a gas pump. Figure 41 shows a schematic and 3D view of the test cell. The final constructed cell is shown by the photograph in figure 42.
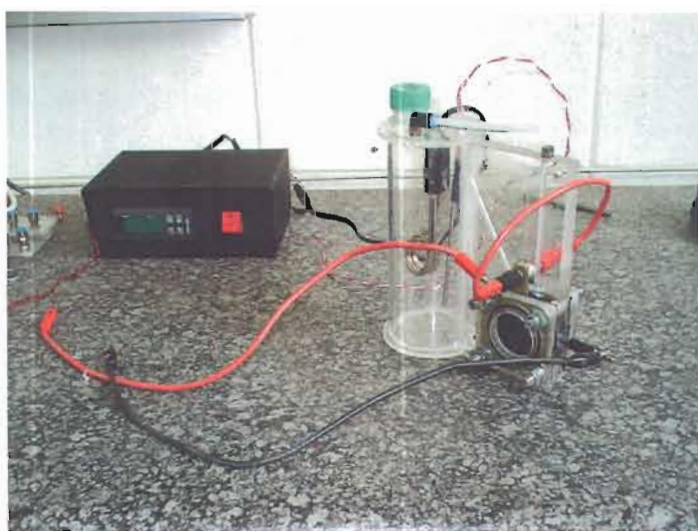
Figure 42: Final constructed test cell.

3.6   Briefing on experiments

The next chapter describes the experiments done on the designed zinc air fuel cell to determine its performance characteristics. The aim was to confirm the capability of a zinc-air fuel cell system to power remote telecommunication systems. The experiments that were done on the zinc-air fuel cell were aimed at:

- Determining the start up time of a freshly fuelled cell.
- Plotting the voltage-current density characteristic of a single zinc-air fuel cell and also the power-current density. These experiments were divided into two separate experiments: (1) Where the cell was at full capacity with freshly added fuel and (2) at 20 percent capacity.

- Showing the difference in power density when using a mobile electrolyte design compared to the static electrolyte design.
- Plotting the discharge curves of the zinc-air fuel cell at different discharge rates to determine the effect it has on fuel efficiency.
- Plotting the voltage-current curves at different operating temperatures.
- Modelling a 100 watt zinc-air fuel cell stack with the results obtained.

3.7   Summary

This chapter defined and explained the design requirements of the zinc-air fuel cell. The additional components needed for the cell to operate successfully were assembled into a complete fuel cell system. Thereafter, a completed prototype refuelling system design was described and reported on. Photographs were included to illustrate where necessary. In the next chapter, the experimental results are given.

Chapter 4 Zinc-air fuel cell experimental test results

4.1 Introduction

The previous chapter presented the design of the zinc-air fuel cell and the additional components necessary for the cell to operate properly. The additional systems and the importance thereof within the fuel cell system were explained. This chapter deals with the experiments preformed on the zinc-air fuel cell. The aim, method and results of each experiment are also given. All experiments were carried out on a single zinc-air fuel cell and the results were used to model a 100 watt zinc-air fuel cell stack. The experiments carried out show the potential of the zinc-air fuel cell and its prospect as a power supply in remote telecommunication systems.

Figure 43 shows a block diagram of the test setup that was used for the experiments reported on. Some components were left out for particular experiments, as these were not always necessary.
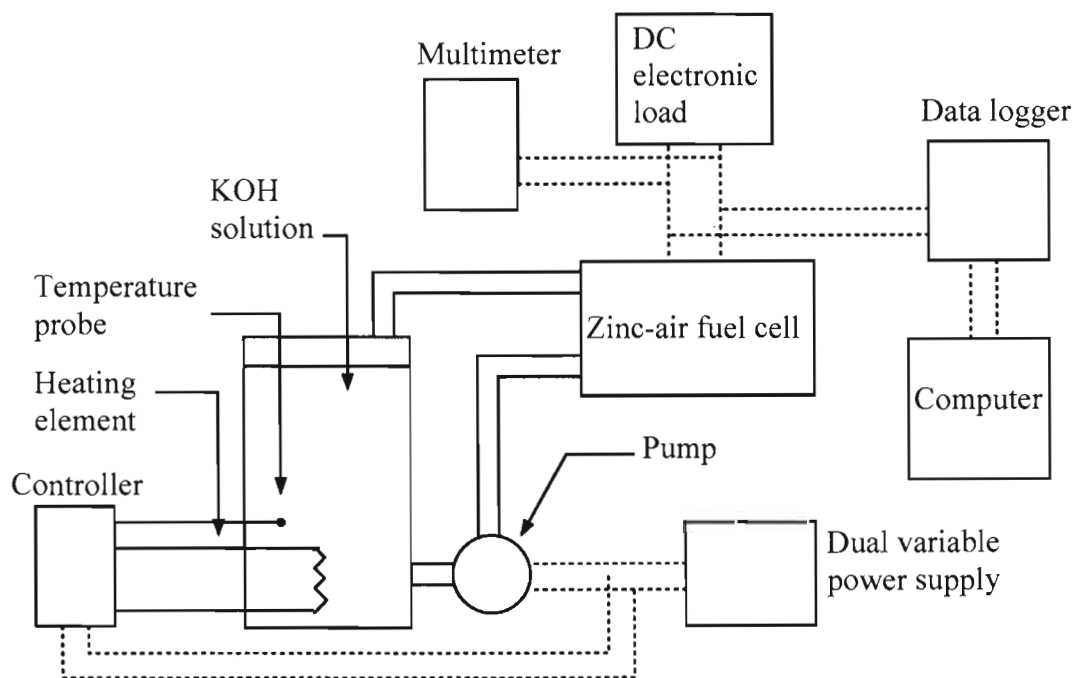
Figure 43: Zinc-air fuel cell test setup.

4.2 Initial cell start-up

The aim of this experiment was to determine the initial duration necessary for the cell to reach full power potential. The results were useful in determining the time needed for the cell to reach full potential in subsequent experiments.

The following equipment was used in the experiment (see figure 43 for setup):

- Zinc-air fuel cell rig
- 28 percent KOH solution
- Dual variable power supply
- Digital multimeters
- DC electronic load
- Electronic data logger

A freshly refuelled cell was connected to an electronic data logger. The electrolyte pump was then started and circulation of the electrolyte through the cell commenced. The voltage of the cell was then recorded against time. The experiment was done to determine the time it takes for the cell to reach its open circuit voltage after start-up. Figure 44 shows the graphical result of the experiment.
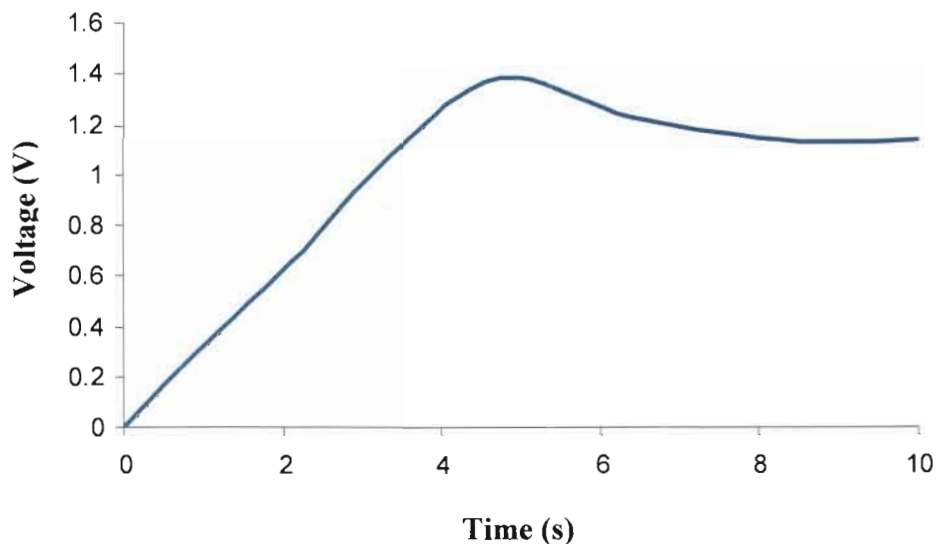
Figure 44: Open circuit voltage characteristic of zinc-air fuel cell at start-up.

The second experiment was done by connecting the cell to the dc electronic load to determine the time necessary for the cell to reach full power potential. The maximum resistive load was applied at intervals of one minute, noting the voltage and current. The data was then used to plot the power curve against time. Figure 45 shows the result of this experiment.
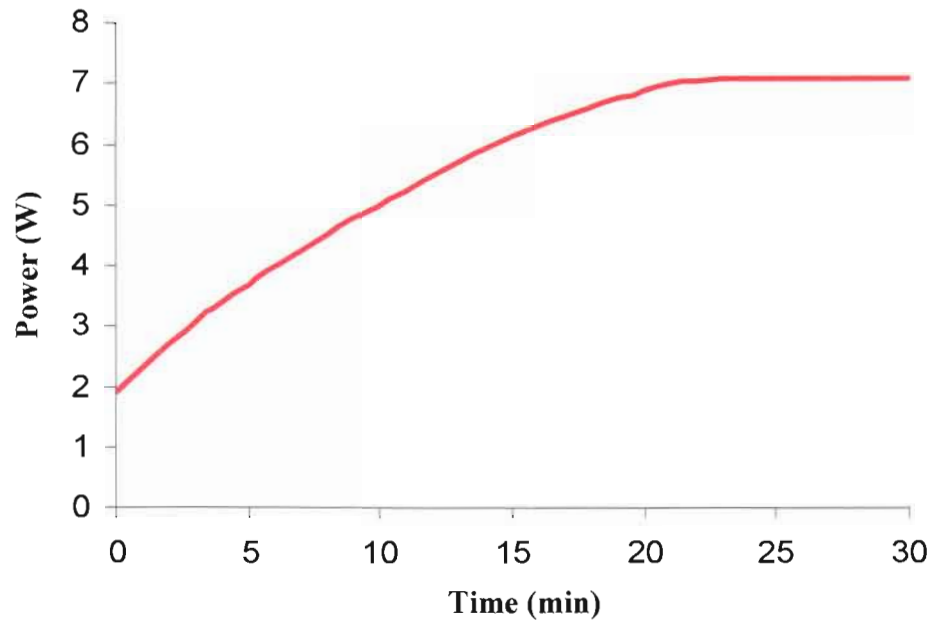
Figure 45: Power potential at different times after first start-up.

Figure 44 shows that the cell reaches full voltage potential in less than ten seconds and figure 45 shows that it takes the same cell almost 25 minutes to reach full power potential. The main reason for this is that the cell requires adequate time for the zinc to absorb the electrolyte. This is a consequence of the density of the zinc particles, which decreases the porosity of the zinc. The use of larger zinc particles or mixing conductive porous spacers with the zinc particles increases the porosity of the zinc and decreases the start-up time. Due to availability, zinc particles of the size used were the only ones available.

4.3 Voltage-current density characteristic curves

The aim of this experiment was to determine the power capability of an individual zinc-air fuel cell at full capacity as well as at 20 percent charge, which can be derived from the voltage-current characteristic curve at both these levels.

The following equipment was used in the experiment (see figure 43 for setup):

- Zinc-air fuel cell rig
- 28 percent KOH solution
- Dual variable power supply
- Digital multimeters
- DC electronic load

The first experiment was done using a freshly refuelled zinc-air fuel cell. The electrolyte was circulated by connecting the dual variable power supply to the electrolyte pump. Circulation through the cell was done for approximately 20 minutes to allow the zinc to absorb the electrolyte and wet the separator material. A voltmeter was connected to the cell to establish whether the cell had reached its open circuit voltage potential. The cell was operated at room temperature.

The zinc-air fuel cell was connected to the DC electronic load, when the cell reached its full potential, measurements on the cell commenced. The DC electronic load was set to present a resistive load that was varied from a low resistance to a high resistance. Voltage measurements were taken while the resistance of the load was increased. The data were recorded and plotted on a graph. For the second experiment, the test was repeated at 20 percent charge. The cell was discharged at a constant current drain of two ampere up to 80 percent depth of discharge, or 0,9 V. This experiment was included to determine the capability of the zinc-air fuel cell to power applications near discharge. Figure 46 shows the data recorded from the two experiments.
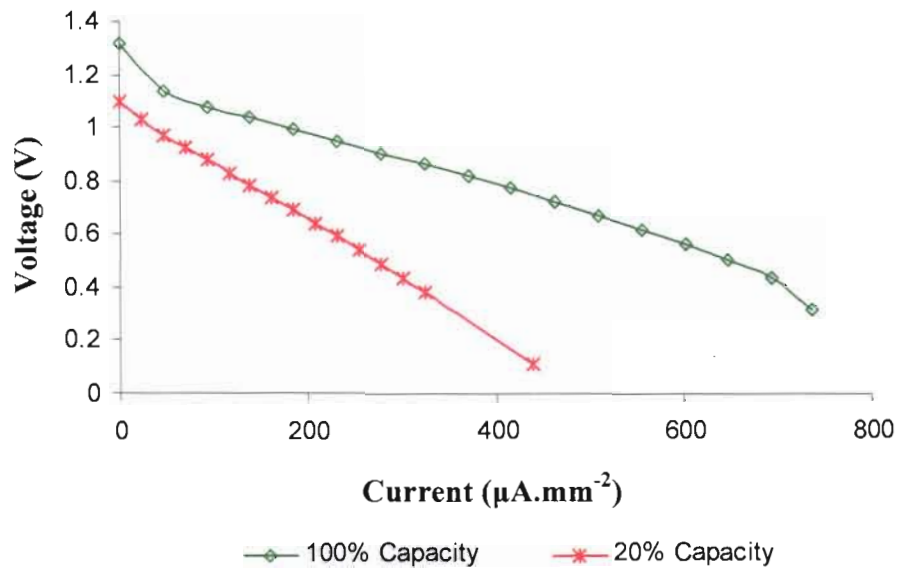
Figure 46: Voltage-current density curve of the zinc-air fuel cell.

The voltage and current data were converted to power density data using the formula:

$$p(t) = v(t) \; x \; i(t) \tag{4.1}$$

These data were then plotted as power density curves in figure 47.
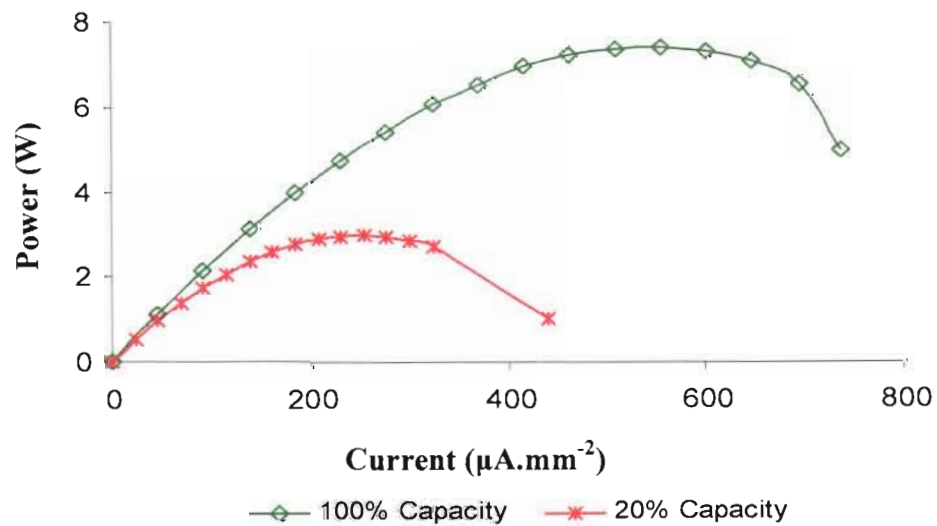
Figure 47: Power-current density characteristic curve.

67

Figure 47 shows the result of the calculations. Maximum power capability is at the point where the power curve reaches maximum curvature. At 100 percent capacity, the maximum power of ~7,8 W was achieved at ~550 μA.mm^{-2}, but at a voltage well below the nominal operating voltage of the zinc-air fuel cell.

The experiments showed the voltage characteristics of a single zinc-air fuel cell and its capability in delivering power to applications at various resistive load levels. Experiment two explored the power capability of the cell at 20 percent charge, demonstrating the ability of the cell to maintain power even in the region of complete discharge. This aspect is important when determining the number of cells necessary to power a particular application (in the case of this research a 100 W telecommunication system).

4.4   Static vs. mobile electrolyte system

The aim of this experiment was to determine the performance difference in the zinc-air fuel cell when using the mobile electrolyte system and static electrolyte system.

The following equipment was used in the experiment (see figure 43 for setup):
- Zinc-air fuel cell rig
- 28 percent KOH solution
- Dual variable power supply
- Digital multimeters
- DC electronic load

The mobile electrolyte data from the previous experiment were used, since the cell made use of the mobile electrolyte system. These data were compared to data obtained from the following static electrolyte experiment.

The static electrolyte experiment was done using a freshly refuelled zinc-air fuel cell. The individual electrolyte input and output connection on the cell was sealed off.

The cell was set aside for approximately 20 minutes to allow the zinc to absorb the electrolyte and wet the separator material. A voltmeter was connected to the cell to establish when the cell had reached its open circuit voltage potential. The cell was operated at room temperature.

The zinc-air fuel cell was connected to the DC electronic load when the cell reached its full potential and measurements commenced. Voltage measurements were taken while the resistance of the load was increased. The data were recorded and plotted on a graph (Figure 48).
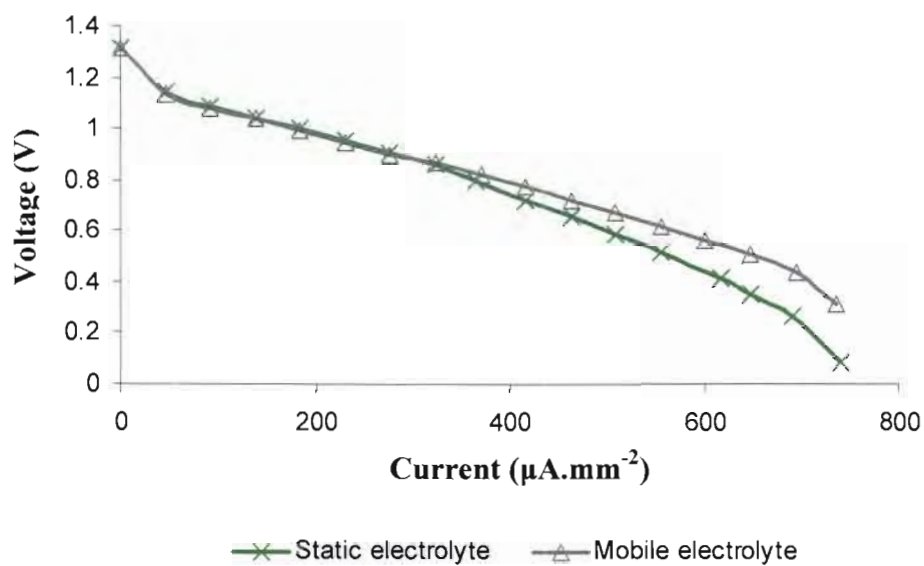
Figure 48: Characteristic curve of the mobile versus static electrolyte system.

The mobile electrolyte system performed better than the static electrolyte system at high discharge rates. The reason is a constant supply of fresh ions in the mobile electrolyte system whereas the main reasons for the reduction in voltage within the static electrolyte design is due to ion depletion at the electrode surface which reduces the rate of the reaction at high discharges. Another reason is the layer of zinc-oxide (ZnO) that grows on the zinc granules at high discharge loads, reducing electrolyte diffusion to the undischarged zinc particles (Kiehne, 2003:21). This is based upon similar electrochemical cells and the process they undergo.

4.5   Cell performance at different operating temperatures

The aim of the experiment was to determine the effect of temperature on the performance of the zinc-air fuel cell. The test was carried out at three predetermined temperature settings; 25 °C, 45 °C and 65 °C.

The following equipment was used in the experiment (see figure 43 for setup):
- Zinc-air fuel cell rig
- 28 percent KOH solution
- Dual variable power supply
- Digital multimeters
- DC electronic load
- Heating element
- Temperature controller

The cell was freshly fuelled and left to stand for the initial start up time required before the experiment commenced for each temperature setting. The electrolyte was circulated by connecting the dual variable power supply to the electrolyte pump. A voltmeter was connected to the cell to establish whether the cell had reached its nominal open circuit voltage potential. Measurements commenced when the cell reached full potential. The heating element was placed in the electrolyte tank. The temperature controller sensor was also placed inside the electrolyte tank. The heating element was connected to the output of the temperature controller and the sensor to the input of the controller.

The first phase of the experiment was carried out at room temperature, 25 °C. The temperature controller was set to 25 °C. The necessary measurements were taken and recorded. For the second phase of the experiment the temperature setting was increased to 45 °C, measurements were taken. In the last phase of the experiment the temperature controller was set to 65 °C and measurements taken. All the results

were plotted on the graph in figure 49 to show the results of temperature variations on the zinc-air fuel cell.
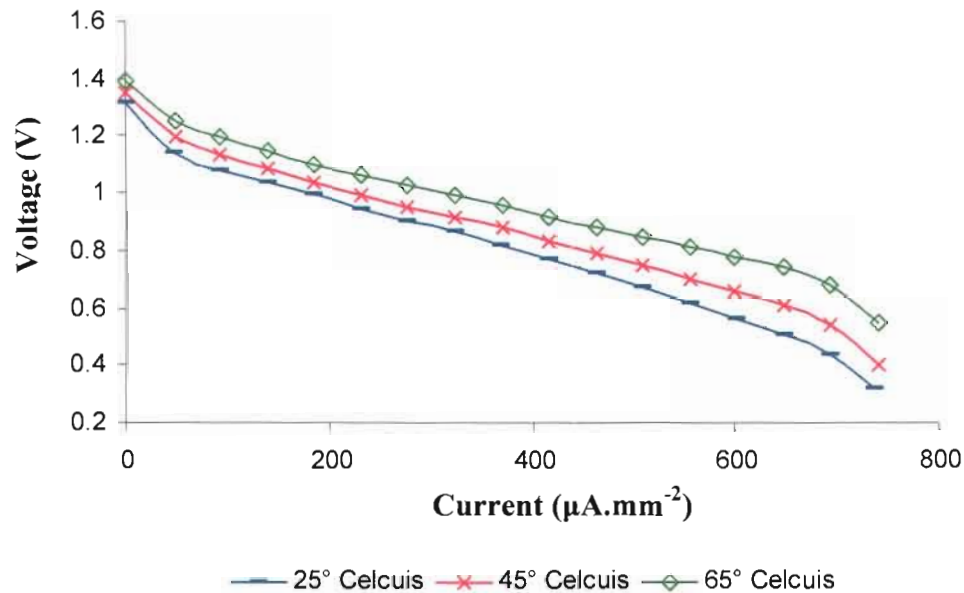
Figure 49: Effects of temperature on the zinc-air fuel cell.

The graph shows that there is a definite increase in cell performance when the cell is operated at higher temperatures. The best results were obtained when the cell was operated at 65 °C. The major reason for the performance increase is that high temperatures increase the catalytic properties of the reactions taking place at the individual electrodes. This is supported by kinetic theory, which states that by heating a mixture or substance, raises the energy levels of the molecules involved in the reaction. Increased temperature means that the molecules move faster. However, high operating temperatures are not practical because water may evaporate, increasing the electrolyte concentration. Moreover, a higher initial start-up time will be present in systems designed to operate at higher temperatures. There will also be increase in cost due to the additional power requirements to heat the system.

A zinc-air fuel cell stack can reach operating temperatures of 40 °C and higher due to the reactions that take place within the cells. This usually happens at high discharge loads. Although there is an increase in stack temperature, the stack is protected

against thermal runaway by the limitation imposed by the rate at which oxygen from the air is consumed by the cell, which limits the current.

4.6   Fuel efficiency at various discharge rates

The aim of this experiment was to determine the effect of high discharge rates on the fuel efficiency and performance of the zinc-air fuel cell. The test was carried out at three different discharge rates; 2 A, 5 A and 8 A.

The following equipment was used in the experiment (see figure 43 for setup):
- Zinc-air fuel cell rig
- 28 percent KOH solution
- Dual variable power supply
- Digital multimeters
- DC electronic load

The cell was freshly fuelled and left to stand for the initial start up time required before the test commenced. The electrolyte was circulated by connecting the dual variable power supply to the electrolyte pump. A voltmeter was connected to the cell to indicate when the cell had reached its nominal open circuit voltage potential. The cell was operated at room temperature. This procedure was followed for all three tests.

The experiment was done by setting the DC electronic load to a constant current drain of 2 A. The load was connected to the cell and only disconnected when cell reached the cut off voltage of 0.9 V. The measured data were recorded. The procedure was then repeated by connecting the DC electronic load to a freshly loaded and readied cell with a constant current drain of 5 A. The cell was again discharged until its cut off voltage and all measured data recorded. The same procedure was repeated by connecting the DC electronic load to a freshly loaded and readied cell

with a constant current drain of 8 A until the cell discharged to its cut off voltage. The measured data were recorded and a graph plotted with the data obtained.
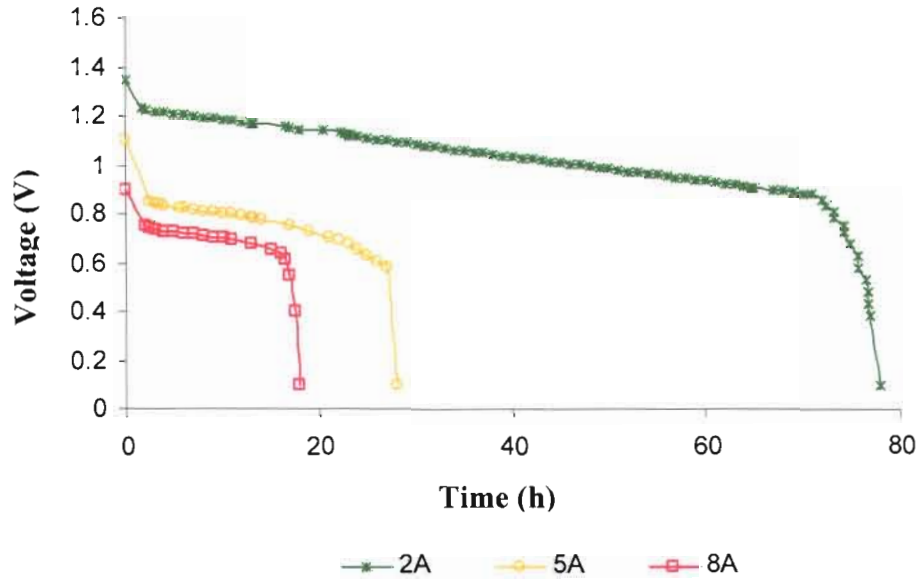
Figure 50: Discharge curve at current drains of 2 A, 5 A and 8A.

The cells were all fuelled with 200 g of zinc particles. The output capacity of a cell can be determined by using the data supplied in Table 1, which show that the energy density of one gram of zinc is equal to 0.8 Ah. The theoretically rated output capacity of the cell can now be determined by the following calculation.

$$Energy_{density} = Weight_{zinc} \times Energy\ Potentail_{zinc} \quad\quad (4.2)$$

$$= 200\ g \times 0.8\ Ah.g^{-1}$$

$$= 160\ Ah$$

The experimental data plotted on figure 50 show a noticeable decrease in both output capacity and voltage with an increase in load. The major reason for the reduction in voltage is ion depletion at the electrode surface, causing a reduction in the reaction

rate. The decreased utilization of the active zinc material is caused by reduction in the diffusion rate. This is caused when some of the undischarged zinc is buried underneath a growing ZnO layer. At high discharged loads this layer grows fast, resulting in a thin but compact covering layer that prevents further reaction or discharge, reducing the overall discharge curve of the cell (Kiehne, 2003:21). The average power obtained from each cell was calculated using the data obtained.

$$Power_{Avg.} = Voltage_{Avg.} \times Current_{Load} \times time\,(hour) \qquad (4.3)$$

$$Power_{2A\ Cell} = 0,986 \times 2 \times 78$$

$$= 153,8\ Wh$$

$$Power_{5A\ Cell} = 0,746 \times 5 \times 28$$

$$= 104,4\ Wh$$

$$Power_{8A\ Cell} = 0,656 \times 8 \times 18$$

$$= 94,5\ Wh$$

Since the theoretical specific energy of zinc is 1352,8 Wh.kg^{-1} (as calculated in section 2.4.2, equation 2.10), the efficiencies of the cell at the different discharge loads can be calculated as follows:

$$\eta_{\%} = \frac{Output\ Energy}{Input\ Energy} \times 100 \qquad (4.4)$$

$$\eta_{2A} = 56,8\,\%$$

$$\eta_{5A} = 38,6\,\%$$

$$\eta_{8A} = 34,9\,\%$$

The results of this experiment show that maximum efficiency can only achieved at low current drains because there is a sharp drop in efficiency as the load current increases.

4.7   A 100 Watt zinc-air fuel cell model

The experimental performance data derived from a single cell were extrapolated to formulate an economical and efficient 100 W zinc-air fuel cell model.

The maximum experimentally determined power for on cell was ~7,5 W, which, if a linear extrapolation is assumed, implies that the number of cells required for a 100 W system is :

$$\text{Cells Required} = \frac{\text{System Power}}{\text{Cell power}} \qquad (4.5)$$

$$= \frac{100}{7,5}$$

$$= 14 \text{ Cells (Rounded)}$$

But figure 46 shows that the cell operates well below the nominal operating voltage at these power drains. Figure 50 also support this by showing that if the cells operate at to a large current load, the overall efficiency of the system is reduced. For these reasons the system will be modelled on parameters that will result in maximum efficiency.

The minimum number of cells required in the zinc-air fuel cell stack can only be determined by the power capability of the cells at 20 percent charge, which is the point at which the system will be refuelled. The maximum power capability of a single cell at 20 percent capacity is in the order of 3 W (Figure 47). The number of cells capable of supplying the application with the required power can thus be calculated using formula 4.5:

$$Cells\ Required = \frac{100}{3}$$

$$= 34\ Cells\ \ (Rounded)$$

The stack voltage can now be calculated using the following equation:

$$Stack\ Voltage = Number\ of\ Cells \times Cell\ Potential \tag{4.6}$$

The variation in cell voltage from full charge to discharge (Figure 46), suggests that the operating stack voltage will vary between 40,8 V for a fully charged stack to about 29 V at discharge. Although the 34 cells will be capable of supplying the 100 W at discharge, it does not take into account the current drain during normal operation and fuel usage efficiency. For maximum fuel utilization, the current drain must not exceed 2 A per cell or 92,6 $\mu A.mm^{-2}$ even at discharge (0,9 V). The maximum power load per cell can now be calculated using equation 4.1.

$$Maximum\ Power_{Cell} = 0,9 \times 2$$

$$= 1,8\ W$$

Thus, for a stack that will operate at maximum efficiency, the number of cells needed can be calculated at a maximum power load per cell of 1,8 W, as follows:

$$\text{Cells Required} = \frac{100}{1,8}$$

$$= 56 \text{ Cells (Rounded)}$$

The total energy required to power a 100 W telecommunication system for at least one month can be calculated as follows:

$$\text{Energy} = 100 \text{ W} \times 24 \text{ h} \times \sim 30 \text{ days}$$

$$= 72\,000 \text{ Wh}$$

The amount of zinc required can be calculated using the theoretical specific power density of one kilogram zinc which is 1352,8 Wh.Kg^{-1} (determined in section 2.4.2).

$$\text{Weight}_{zinc} = \frac{72\,000 \text{ Wh}}{1352,8 \text{ Wh.Kg}^{-1}}$$

$$= 53,2 \text{ Kg}$$

The total zinc-air fuel cell system will consist of 56 cells and 53,2 Kg of zinc fuel. A battery bank of the same energy capacity can be calculated using the energy capacity of a single zinc-air battery which is approximately 80 Ah. The power capacity of a single cell is thus:

$$\text{Power}_{Cell} = 80 \text{ Ah} \times 1,2 \text{ V (practical operational voltage)}$$

$$= 96 \text{ Wh}$$

The number of cells required to power the system for one month is thus:

$$\text{Cells Required} = \frac{72\,000}{96}$$

$$= 750\,\text{Cells}$$

It is clear from the calculations that a fuel cell system will require far less cells, reducing both cost and maintenance.

4.8   Summary

This chapter explored the performance characteristics of a single zinc-air fuel cell under varying conditions. The results of these experiments were used to model a 100 W zinc-air fuel cell stack that can be used in telecommunication systems. It showed that fewer cells are required compared to a battery bank. In the next chapter, conclusions will be drawn with regards to the results obtain from this research. Recommendations and suggestions for further research will also be presented.

Chapter 5   Conclusion

5.1 Introduction

This chapter draws conclusions with regards to the design and development of a high performance zinc-air fuel cell and the results obtained. Recommendations regarding the design and possible solutions to problems encountered within the research are also discussed. The chapter ends with suggestions for future research that may be of benefit to the technology.

5.2 Conclusions

It was found that zinc particles in conjunction with a metal current collecting grid could be used in both zinc-air batteries and fuel cells as opposed to the solid porous electrodes commonly used in the zinc-air cell. Although the cell design was successful, there are still problems with the refuelling of the cell as well as constant leaking of the aqueous electrolyte through the refuelling mechanisms. It was also observed that the zinc particles bonded to each other as the cell was discharged. The major reason being that the electrolyte circulation was not effective enough in washing away the spent product, eventually clogging the cell. Figure 51 shows a photograph of how the particles clogged together to form a solid structure.

Figure 51: Solid zinc structure.

The cell performed well at low current drains (less than 200 μA.mm^{-2}) but suffered severely at high current drains (more than 200 μA.mm^{-2}), lowering the overall efficiency of the system. The performance of the proposed fuel cell design showed that there will be a definite reduction in both cost and maintenance when comparing the fuel cell system design to that of a battery bank. Through calculations it was shown in section 4.7 that for the system to operate at maximum efficiency, the zinc-air fuel cell stack should consist of about 56 cells.

Unlike zinc-air batteries that suffer from drying due to electrolyte evaporation, the zinc-air fuel cell did not have these problems due to a constant circulation of the electrolyte.

5.3 Recommendations

Although acceptable rotation was achieved through the gear and chain connection at the fuelling mechanism, it could prove more useful to replace the chain by a worm screw. The worm screw is directly connected to the motor. The screw will be placed over the gears that are connected to the fuelling mechanism. As the worm screw rotates, so will the gear that is connected to the fuelling mechanism, achieving full rotation. This will reduce the space occupied by the mechanism. Figure 52 shows a illustration of the worm screw and gear.

Worm screw

Gear
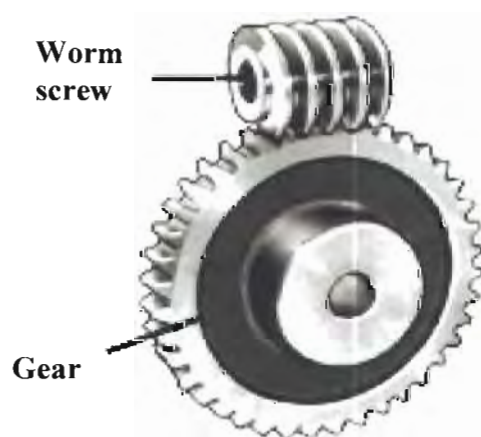
Figure 52: Proposed driving unit for fuelling mechanism.

Designing the fuelling mechanism posed many problems due to the nature of both the fuel as well as the electrolyte. Persistent leakage occurred throughout testing due to the extremely low surface tension of the electrolytic solution. The simplest solution to this problem is to change the cell design from the two fuelling mechanisms to only one at the top. This will prevent any leaking at the bottom of the cell. The fuel cell stack and auxiliary systems connected to the stack can all be built into a rotating cage. At refuelling, the entire fuel cell stack will be rotated upside down, at which stage the refuelling mechanism is turned on and the discharged zinc is removed. After this, the stack is returned to its upright position and refuelled. Figure 53 shows a graphic representation of the proposed modification.
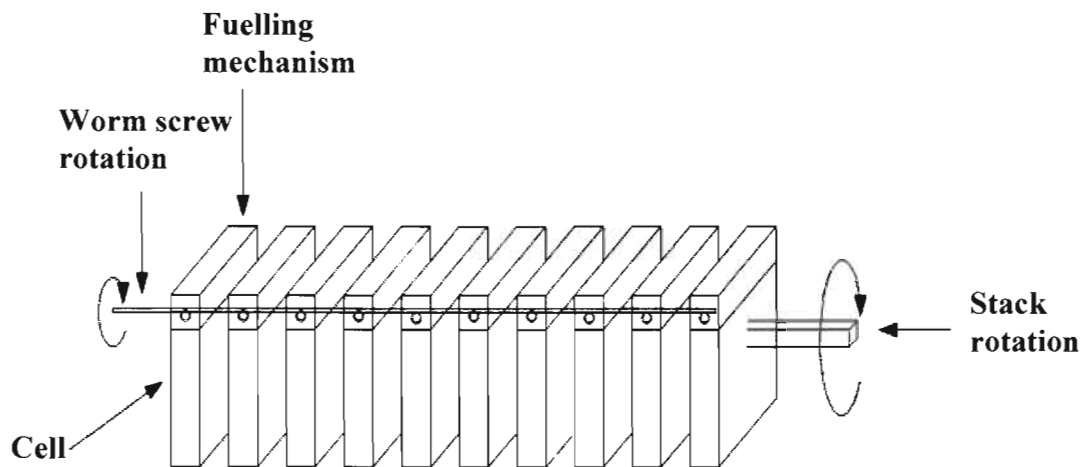
Figure 53: Graphic representation of modified fuel cell stack.

It will also be beneficial to use mono-air electrodes instead of bi-functional electrodes as used in the experimental design. Mono-air electrodes have the benefit of being both lighter and thinner, and in reducing the transport hindrances within the electrode structure. This will increase the power density of the cell, due to lower polarization losses.

5.4 Fields for further research

This work suggests that the following may prove to be useful avenues for future research. A major disadvantage in all fuel cell systems currently in development is the series connection of the individual cells within the stack, which poses a problem when one of these cells fail, breaking the circuit.

An interesting study could be the use of hydrogen gas for recharging of the discharged zinc-air cell. Clarke and Wasson (1984:223) explain that feeding hydrogen gas to the anode of a zinc powder cell is exactly the same process as consuming hydrogen gas at the anode of a hydrogen fuel cell. The only difference is that zinc is produced at the cathode as a by- product; this reaction replaces the air electrode in a fuel cell. The advantage of a system like this is that power can be drawn from the system during both discharge and charge. The zinc-air fuel cell will discharge as described throughout this dissertation, but when the cell is fully discharged, the discharged zinc, or zinc-oxide will again be converted back to zinc through the hydrogen reaction, producing power. When all the zinc-oxide is converted to zinc, the cell again can operate as normal.

BIBLIOGRAPHY

BECK, F. & RÜETSCHI, P. 2000. Rechargeable batteries with aqueous electrolytes. *Electrochimica Acta*, 45(2467-2482). [Online]. Available at: <http://www.sciencdirect.com/>. Accessed: 01/12/2005.

BENDER, S.F., CRETZMEYER, J.W. & REISE, T.F. 1995. Zinc/Air cells. Chapter 13. In LINDEN, D. *Handbook of batteries*. 2nd ed. New York. McGraw-Hill.

BERNDT, D. 1997. *Maintenance-Free batteries*. 2nd ed. Somerset. John Wiley and Sons Ltd.

BRODD, R.J. 1999. Recent developments in batteries for portable consumer electronics applications. *The Electrochemical Society Interface*, 8(20-23). [Online] Available at: <http://www.electrochem.org/>. Accessed: 29/10/2005.

BUDEVSKI, E. 2003. Structural aspects of fuel cell electrodes. *Journal of Optoelectronics and Advanced Materials*. Volume 5. No.5(1319-1325). [Online]. Available at: <http://joam.infim.ro/>. Accessed: 25/5/2005.

BURGER, H. 2005. January 20. Subject: KOH conductivity curve. [Online]. Personal E-mail from H. Burger, Kumba Resources <hennie.burger@kumbaresources.co.za>.

CAIRNS, E J. 2003. Aqueous carbonate electrolyte fuel cells. Chapter 17. In VIELSTICH, W., LAMM, A. & GASTEIGER, H A. *Handbook of Fuel Cells*. Volume 1. Sussex: John Wiley & Sons Ltd.

CHAKKARAVARTHY, C., ABDUL WAHEED, A.K. & UDUPA, H.V.K. 1981. Zinc-Air alkaline batteries- A review. *Journal of Power Sources*, 6(203-228).

IOWA STATE UNIVERSITY. 2002. Material safety data sheets. [Online]. Available at: <http://avogadro.chem.iastate.edu/MSDS/KOH.htm> Accessed: 30/06/2006.

CLARKE, R.L. & WASSON, A.R. 1984. Zinc-air-hydrogen; an alternative battery system for electric vehicles. *Extended abstracts,* (222-224)

COLBORN, J. & SMEDLEY, S. 2001. Ultra-long duration backup for telecommunications applications using zinc/air regenerative fuel cells. *Telecommunications Energy Conference.* Twenty-third international, (576-581). [Online]. Available at: <http://intl.ieeexplore.ieee.org/ >. Accessed: 14/06/2005.

DEWI, E.L., OYAIZU, K., NISHIDE, H. & TSUCHIDA, E. 2003. Cationic polysulfonium membrane as separator in zinc-air cell. *Journal of Power Sources,* 115(149-152).

DOBLEY, A., DICARLO, J. & ABRAHAM, K.M. 2005. Non-aqueous lithium-air batteries with advanced cathode structure. [Online] Available at: <http://www.yardney.com/>. Accessed : 11/24/2005.

DYER, C.K. 2002. Fuel cells for portable applications. *Journal of Power Sources,* 106(31-43).

EDUGREEN.TERI.RES.IN. 2006. Fuel cells. [Online]. Available at: <http://edugreen.teri.res.in/explore/renew/fuelcell.htm> Accessed: 30/06/2006.

ELECTRIC-FUEL.COM. 1995. Electric fuel zinc-air battery regeneration technology. [Online]. Available at: <http://www.electric-fuel.com/>. Accessed: 13/03/2005.

EWELS, C. 2005. *Image Gallery – Nanotubes.* [Online]. Available at: <http://www.ewels.info/img/science/nanotubes/>. Accessed: 19/10/2005.

HAAS, O., HOLZER, F., MÜLLER, K. & MÜLLER, S. 2003. Metal/air batteries: The zinc/air case. Chapter 22. In VIELSTICH, W., LAMM, A & GASTEIGER, H.A. *Handbook of Fuel Cells*. Volume 1. Sussex: John Wiley & Sons Ltd.

JENA, A., SANDERS, H., MILLER, J. & WIMBERLY, R. 2001. Comparison of mercury porosimetry and flow porometry for the testing of battery separator materials. *IEEE*, (71-75)
[Online] Available at: <http://ieeexplore.ieee.org/>. Accessed: 04/01/2006.

JIANG, Z. & CINTRA, G. 2005. *Zinc/air cell with improved anode*. Agent Barry D. Josephs Attorney At Law, (patent 20050003271). [Online]. Available at: <http://www.freshpatents.com/>. Accessed: 24/01/2005.

KAISHEVA, A. 2004. Comparative methods for gas-diffusion electrodes diagnostics. *Institute of Electrochemistry and Energy Systems. Bulgarian Academy of Sciences* [Online]. Available at: <http://www.bas.bg/cleps/workshop/program/posters/paper-kaisheva.pdf>. Accessed: 08/09/2005

KAISHEVA, A. & MILUSHEVA, J. 2004. Methods for investigation of pyrolyzed COTMMPP catalysts. *Bulgarian Academy of Sciences*. [Online]. Available at: <http://www.bas.bg/>. Accessed: 10/4/2005

KIEHNE, H.A. 2003. *Battery technology handbook*. New York. M. Dekker.

KORDESCH, K. & HACKER, V. 2003. Stack materials and design. Chapter 56. In VIELSTICH, W., LAMM, A & GASTEIGER, H.A. *Handbook of Fuel Cells*. Volume 4. Sussex: John Wiley & Sons Ltd.

LARMINIE, J. & DICKS, A. 2003. *Fuel cell systems explained*. 2nd ed. Sussex: John Wiley and Sons Ltd.

NAIMER, N., KORETZ, B. & PUTT, R. 2002. Zinc-air batteries for UAVs and MAVs. *Electric Fuel*. [Online]. Available at: <http://www.electric-fuel.com/>. Accessed: 18/12/2005.

PACKAGINGTODAY.COM. 2006. An Introduction to the History of Plastics & Plastic Packaging Products. [Online]. Available at: <http://www.packagingtoday.com/introplasticexplosion.htm>. Accessed: 18/03/2006.

PESCOVITZ, D. 2002. *The Tinkertoys of Nanotechnology*. [Online]. Available at: <http://www.coe.berkeley.edu/labnotes/0702/zettl.html>. Accessed: 19/10/2005.

PUTT, R.A. & WOODRUFF, G. 1993. Advanced zinc-air batteries. *American Chemical Society*, 1(1085-1089).

SCOTT, D.S. 2004. Inside fuel cells. *International Journal of Hydrogen Energy*. 29(1203-1211).

SITE.GREENBATTERIES.COM. 2006. New technology batteries guide. [Online]. Available at: <http://site.greenbatteries.com/batteryguide.html>. Accessed: 09/01/2006.

SMITH, G. 1980. *Storage batteries including operation, charging, maintenance and repair*. London. Pitman.

STU.INONU.EDU.TR. 2005. Zinc/air cells. [Online]. Available at: <http://stu.inonu.edu.tr/>. Accessed: 16/08/2005.

SURESH KANNAN, A.R., MURALIDHARAN, S., SARANGAPANI, K.B., BALARAMACHANDRAN, V. & KAPALI, V. 1995. Corrosion and anodic behaviour of zinc and its ternary alloys in alkaline battery electrolytes. *Journal of Power Sources*, 57(93-98).

METALLICPOWER.COM. 2004. Fuel cell technology. [Online]. Available at: <http://www.metalicpower.com/>. Accessed: 06/09/2004.

VINCENT, C.A. & SCROSATI, B. 1997. *Modern Batteries.* 2nd ed. New York. Butterworth-Heinemann.

WEI, Z., HUANG, W., ZHANG, S. & TAN, J. 2000. Carbon-based air electrodes carrying MnO_2 in zinc-air batteries. *Journal of Power Sources,* 91(83-85).

WORTH, B., PERUJO, A. & DOUGLAS, K. 2002. *Investigation on storage technologies for intermittent renewable energies*: Evaluation and recommended R&D strategy. [Online]. Available at: <http://www.itpower.co.uk/>. Accessed: 17/12/2005.

ZHU, W.H., POOLE, B.A., CAHELA, D.R. & TATARCHUK, B.J. 2003. New structures of thin air cathodes for zinc-air batteries. *Journal of Applied Electrochemistry,* 33(29-36).

Annexure A   Cell characterization

The aim of this experiment was to determine the V-I curve of an 80Ah zinc-air cell in order to characterize the electrical performance of the cell.

The setup for this experiment was done with the following equipment as shown in figure 54.

- 80 Ah electrically rechargeable zinc-air cell.
- DC electronic load
- Digital multimeter
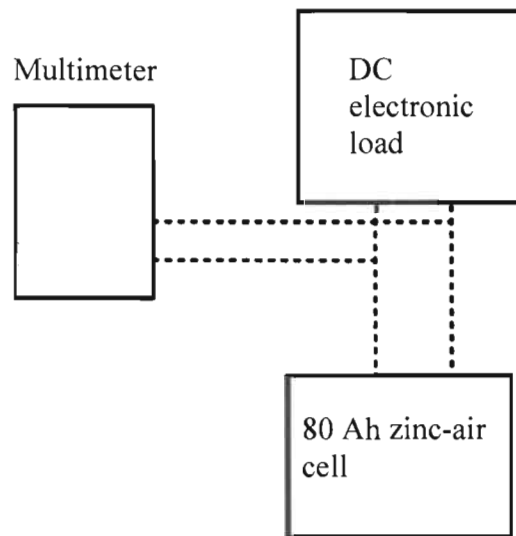
Figure 54: Cell characterization test setup

Using a new cell, the experiment was done by filling it with fresh electrolyte and allowing time for the zinc electrode to soak up the electrolyte. When the open circuit voltage (OCV) reached the practical potential for a cell, the DC load was connected. The load current was increased by 500 mA, the voltage was noted at each of the increments. Table 2 shows the data obtained from the experiment, from this the V-I curve can be established.

Table 2: Measured data of cell

	Cell voltage (V)	Current (A)	Current (mA.cm⁻²)
1	1.399	0	0.00
2	1.19	0.92	4.26
3	1.163	1.13	5.23
4	1.14	1.5	6.94
5	1.127	2	9.26
6	1.111	2.5	11.57
7	1.097	3	13.89
8	1.085	3.5	16.20
9	1.074	4	18.52
10	1.059	4.5	20.83
11	1.047	5	23.15
12	1.035	5.5	25.46
13	1.023	6	27.78
14	1.011	6.5	30.09
15	0.999	7	32.41
16	0.988	7.5	34.72
17	0.977	8	37.04
18	0.965	8.5	39.35
19	0.952	9	41.67
20	0.938	9.5	43.98
21	0.927	10	46.30
22	0.915	10.5	48.61
23	0.903	11	50.93
24	0.891	11.5	53.24
25	0.879	12	55.56
26	0.869	12.5	57.87
27	0.857	13	60.19
28	0.847	13.5	62.50
29	0.837	14	64.81
30	0.827	14.5	67.13
31	0.818	15	69.44
32	0.807	15.5	71.76
33	0.797	16	74.07
34	0.783	16.5	76.39
35	0.777	17	78.70
36	0.767	17.5	81.02
37	0.757	18	83.33
38	0.747	18.5	85.65
39	0.733	19	87.96
40	0.723	19.5	90.28
41	0.71	20	92.59
42	0.7	20.5	94.91
43	0.691	21	97.22
44	0.68	21.5	99.54
45	0.67	22	101.85
46	0.659	22.5	104.17

47	0.649	23	106.48
48	0.639	23.5	108.80
49	0.607	24.15	111.81
50	0.36	27	125.00

Annexure B   Discharge characteristics of a zinc-air cell

The aim of this experiment is to determine the discharge curve of the 80 Ah zinc-air cell.

The experiment was done with the following equipment as shown in figure 55.
- 80 Ah electrically rechargeable zinc-air cell.
- DC electronic Load
- Digital multimeter
- Data logger
- Computer
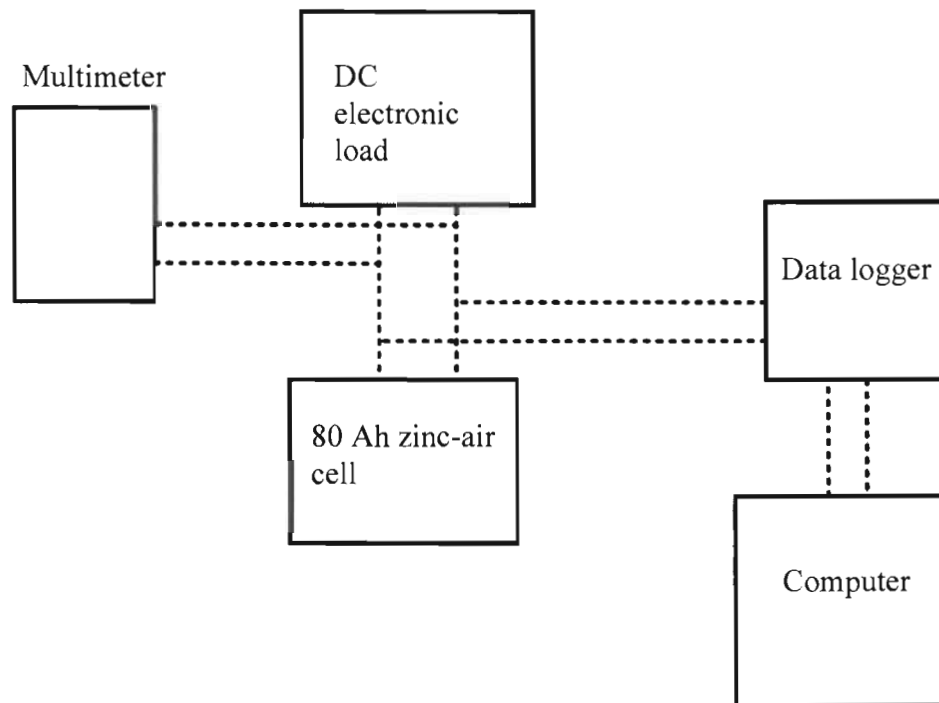
Figure 55: Discharge characterization test setup

Using a new cell, the experiment was done by filling it with fresh electrolyte and allowing the zinc electrode to soak up the electrolyte. The OCV was noted and when the cell reached its practical potential the DC electronic load as well as the data logger was connected. The experiment was continued by constantly discharging the

cell at a constant one ampere hour and until fully discharged. The voltage measurement was logged every 1 minute. The result of this experiment is shown in the table below.

Table 3: Data obtained from data logger

	Voltage(V)	Time (h)
1	1.4	0
2	1.118	1
3	1.118	2
4	1.118	3
5	1.118	4
6	1.118	5
7	1.129	6
8	1.118	7
9	1.118	8
10	1.129	9
11	1.129	10
12	1.118	11
13	1.118	12
14	1.129	13
15	1.118	14
16	1.118	15
17	1.118	16
18	1.118	17
19	1.118	18
20	1.118	19
21	1.118	20
22	1.118	21
23	1.118	22
24	1.118	23
25	1.118	24
26	1.106	25
27	1.118	26
28	1.118	27
29	1.118	28
30	1.106	29
31	1.106	30
32	1.106	31
33	1.106	32
34	1.106	33
35	1.106	34
36	1.094	35
37	1.094	36
38	1.094	37
39	1.094	38
40	1.082	39

41	1.082	40
42	1.082	41
43	1.082	42
44	1.071	43
45	1.071	44
46	1.071	45
47	1.071	46
48	1.059	47
49	1.059	48
50	1.059	49
51	1.047	50
52	1.047	51
53	1.035	52
54	1.047	53
55	1.035	54
56	1.035	55
57	1.024	56
58	1.024	57
59	1.024	58
60	1.012	59
61	1	60
62	1	61
63	0.976	62
64	0.965	63
65	0.965	64
66	0.953	65
67	0.953	66
68	0.929	67
69	0.918	68
70	0.906	69
71	0.894	70
72	0.871	71
73	0.847	72
74	0.8	73
75	0.682	74
76	0.529	75
77	0.282	76
78	0	77

Annexure C   Temperature variations on discharge capacity

The aim of this experiment was to determine the effect that temperature has on the discharge capacity of the 80 Ah zinc-air cell. The experiment was carried out by a fellow Masters student, Petros Mandla Sibiya, project title: Analysis of environmental impact on the design of fuel cells.

The setup for these experiments was done with the following equipment as shown in figure 56.

- 80 Ah electrically rechargeable zinc-air cell.
- Temperature and humidity controllable chamber
- Digital multimeter
- DC electronic load
- Data logger
- Computer
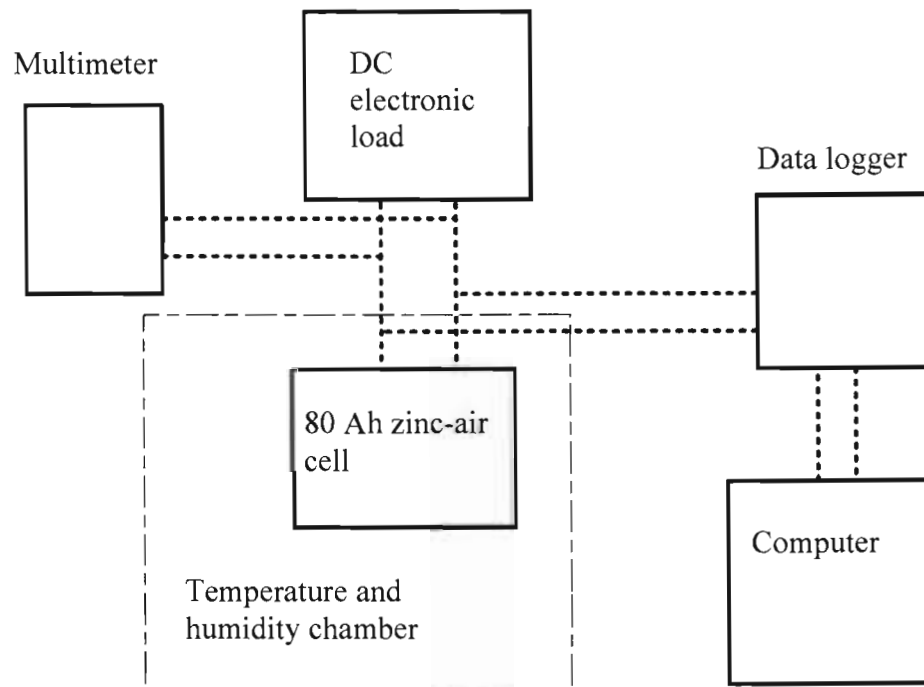
Figure 56: Temperature variation test setup

The effect that temperature has on the discharge capacity of the cell was determined at the following temperatures, -20, 20, 40, 60 and 70 degrees Celsius, at relative humidity (RH) 50 percent. The cell was discharged at a constant two ampere until fully discharge. The results of these experiments can be seen in the table below.

Table 4: Measured discharge data at various temperatures

	Cell voltage (V) @ -20 °C (50% RH)	Cell voltage (V) @ 20 °C (50% RH)	Cell voltage (V) @ 40 °C (50% RH)	Cell voltage (V) @ 60 °C (50% RH)	Cell voltage (V) @ 70 °C (50% RH)
1	0.812	1.082	1.118	1.118	1.129
2	0.776	1.082	1.129	1.129	1.129
3	0.765	1.094	1.118	1.141	1.129
4	0.765	1.082	1.129	1.118	1.118
5	0.753	1.094	1.118	1.118	1.106
6	0.729	1.082	1.129	1.153	1.082
7	0.706	1.082	1.129	1.153	1.071
8	0.682	1.082	1.118	1.153	1.024
9	0.647	1.071	1.118	1.165	0.941
10	0.624	1.071	1.106	1.153	0.871
11	0.576	1.059	1.106	1.153	0.741
12	0.529	1.059	1.106	1.153	0.388
13	0.471	1.059	1.094	1.153	0.012
14	0.412	1.047	1.094	1.153	0
15	0.341	1.047	1.082	1.141	
16	0.2	1.047	1.094	1.141	
17	0	1.047	1.082	1.129	
18		1.047	1.082	1.118	
19		1.012	1.082	1.082	
20		1.012	1.082	1.059	
21		1.012	1.071	1	
22		1	1.071	0.918	
23		1.012	1.071	0.718	
24		1.012	1.071	0.694	
25		1.012	1.071	0	
26		1	1.071		
27		1	1.047		
28		1	1.047		
29		0.988	1.024		
30		0.976	1.012		
31		0.965	0.988		
32		0.953	0.953		
33		0.941	0.918		
34		0.918	0.835		
35		0.906	0.635		
36		0.906	0.024		
37		0.882	0		

38		0.871			
39		0.859			
40		0.824			
41		0.788			
42		0.718			
43		0.494			
44		0.035			
45		0			

Annexure D   PIC flow code

Using Analogue inputs

```
BEGIN
  │
  ▼
 Loop
 While 1
  │
  ▼
Read the analogue value
SampleADC
  │
  ▼
Store the hi-byte value
ReadHigh
  │
  ▼
Decision
HI>=205?  ──Yes──►
  │
  No
  ▼
Decision
HI>=154?  ──Yes──►
  │
  No
  ▼
Output
48 -> PORT D
```

A: Connection Point A

```
INPUT   Input
        S1 <- PORT D
  │
  ▼
Decision
S1=4?  ──Yes──►
  │
  No
  ▼
Decision
S1=0?  ──Yes──►
  │
  No
  ▼
 A   Goto Connection Point A
```

```
OUTPUT   Output
         0 -> PORT D
  │
  ▼
DELAY    Delay
         300 ms
  │
  ▼
B:   Connection Point B
  │
  ▼
INPUT    Input
         S2 <- PORT D
  │
  ▼
Decision
S2=8?  ──Yes──►
  │
  No
  ▼
Decision
S2=0?  ──Yes──►
  │
  No
  ▼
 B   Goto Connection Point B
```

```
OUTPUT   Output
         0 -> PORT D
```

```
DELAY   Delay
        200 ms
  │
  ▼
 Loop
  │
  ▼
 END
```

97